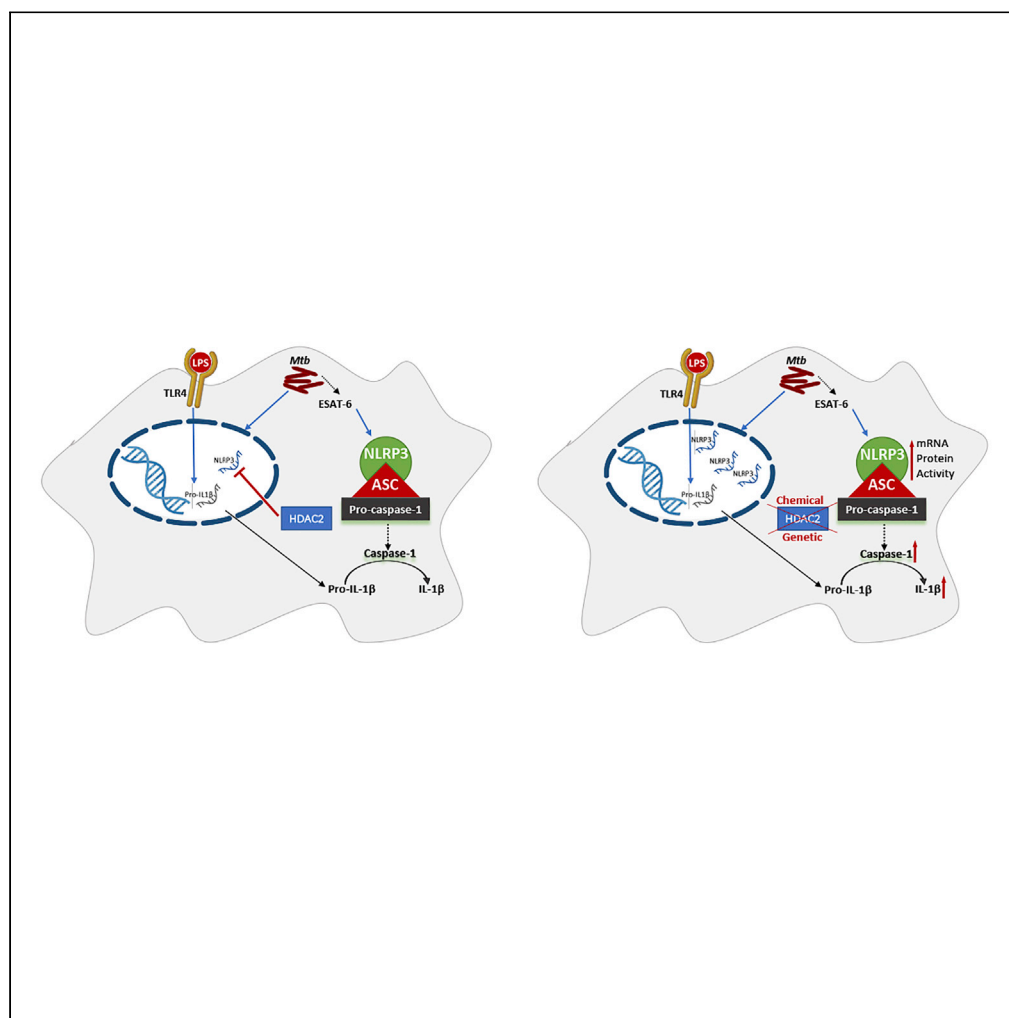


Article

Histone deacetylase-2 controls IL-1 β production through the regulation of NLRP3 expression and activation in tuberculosis infection

Jôsimar Dornelas
Moreira, Alexei
Iakhiaev,
Ramakrishna
Vankayalapati,
Bock-Gie Jung,
Buka Samten

buka.samten@uthct.edu

Highlights

HDAC1 inhibitor, DHOB, increased IL-1 β production via NLRP3 inflammasome activation

DHOB suppressed deacetylase activities of both HDAC1 and HDAC2 by direct interaction

Deletion of HDAC2, but not HDAC1, increased IL-1 β production by increased NLRP3 expression

DHOB increased IL-1 β and NLRP3 expression in a mouse model of TB infection

Moreira et al., iScience 25,
104799
August 19, 2022 © 2022 The
Author(s).
[https://doi.org/10.1016/
j.isci.2022.104799](https://doi.org/10.1016/j.isci.2022.104799)

Article

Histone deacetylase-2 controls IL-1 β production through the regulation of NLRP3 expression and activation in tuberculosis infectionJôsimar Dornelas Moreira,¹ Alexei Iakhsiev,² Ramakrishna Vankayalapati,¹ Bock-Gie Jung,¹ and Buka Samten^{1,3,*}

SUMMARY

Histone deacetylases (HDACs) are critical immune regulators. However, their roles in interleukin-1 β (IL-1 β) production remain unclear. By screening 11 zinc-dependent HDACs with chemical inhibitors, we found that HDAC1 inhibitor, 4-(dimethylamino)-N-[6-(hydroxyamino)-6-oxohexyl]-benzamide (DHOB), enhanced IL-1 β production by macrophage and dendritic cells upon TLR4 stimulation or *Mycobacterium tuberculosis* infection through IL-1 β maturation via elevated NLRP3 expression, increased cleaved caspase-1, and enhanced ASC oligomerization. DHOB rescued defective IL-1 β production by dendritic cells infected with *M. tuberculosis* with ESAT-6 deletion, a virulence factor shown to activate NLRP3 inflammasome. DHOB increased IL-1 β production and NLRP3 expression in a tuberculosis mouse model. Although DHOB inhibited HDAC activities of both HDAC1 and HDAC2 by direct binding, knockdown of HDAC2, but not HDAC1, increased IL-1 β production and NLRP3 expression in *M. tuberculosis*-infected macrophages. These data suggest that HDAC2, but not HDAC1, controls IL-1 β production through NLRP3 inflammasome activation, a mechanism with a significance in chronic inflammatory diseases including tuberculosis.

INTRODUCTION

Tuberculosis (TB), a chronic pulmonary infection of *Mycobacterium tuberculosis* (*Mtb*), remains as a major cause of human death due to continuous development of drug resistance by *Mtb* (WHO, 2018). Therefore, it is crucial to design novel host-directed therapeutics (HDT) that target human (host) genes and mechanisms rather than those of the pathogen to complement and improve the current TB therapy. Therefore, understanding the molecular mechanisms of interactions between host and pathogen will help identify host molecular and cellular pathways for the development of HDT for the improved management of TB by the prevention of the drug resistance development by *Mtb*.

It is evident that intracellular bacteria can manipulate host immune cell responses by changing chromatin structure and thereby transcriptional responses of critical immune response genes via a variety of epigenetic regulatory mechanisms, such as histone modifications, DNA methylation, chromatin-associated complexes, noncoding RNAs, and RNA splicing factors (Arbibe et al., 2007; Bierne et al., 2012; Garcia-Garcia et al., 2009; Hamon and Cossart, 2011; Moreira et al., 2020; Patel et al., 2017). It has recently been identified that several intracellular pathogens including *Mtb* manipulate host cell antibacterial immune responses for their immune evasion by acetylation of the histones and nonhistone proteins (Ding et al., 2010; Savelyeva and Dobbelstein, 2011; Wang et al., 2005; Wu et al., 2010). Histone acetyltransferases (HATs) catalyze the transfer of an acetyl group from acetyl coenzyme A to the histone N-terminal tails, resulting in a relaxed chromatin, which is associated with transcriptional activation of the target genes by increased accessibility of the regulatory units of target genes to the transcriptional machinery. In contrast, histone deacetylases (HDACs) catalyze the removal of acetyl groups from the lysine residues of the histones, resulting in condensed chromatin structure, which is associated with transcriptional repression.

There are 18 histone deacetylases (HDACs) that are divided into four classes: class I (HDAC1, 2, 3, and 8), class II including class IIa (HDAC4, 5, 7, and 9) and class IIb (HDAC6 and 10), class III (SIRT1-7), and class IV (HDAC11) based on their function, co-factor dependency, and structural homology to yeast HDACs. Class I,

¹Department of Pulmonary Immunology, The University of Texas Health Science Center at Tyler, Tyler, TX, USA

²Division of Natural & Computational Sciences, Texas College, 2404 North Grand Avenue, Tyler, TX 75702, USA

³Lead contact

*Correspondence: buka.samten@uthct.edu
<https://doi.org/10.1016/j.isci.2022.104799>



II, and IV HDACs have a zinc-dependent active site, whereas class III proteins are dependent on NAD⁺ for their catalytic activities (Park and Kim, 2020).

HDACs play critical roles in the expression of host defense genes, including pattern-recognition receptors (PAMPs), kinases, transcriptional regulators, and cytokines (Nusinzon and Horvath, 2003; Roger et al., 2011). Pan-HDAC inhibitors enhance production of a subset of pro-inflammatory cytokines including interleukin (IL)-1 β and other inflammatory mediators (Cox et al., 2020; Seshadri et al., 2017); nevertheless, the precise roles of HDACs in immune regulation remain unclear.

Interleukin-1 β (IL-1 β) is a potent pro-inflammatory cytokine, and the defects in IL-1 β pathway are associated with increased TB-susceptibility in both patients (Bellamy et al., 1998; Wilkinson et al., 1999) and mouse models (Fremond et al., 2007; Juffermans et al., 2000; Mayer-Barber et al., 2010). However, excess IL-1 β production may also be detrimental to the host due to inflammation and lung damage (Mishra et al., 2013; Zhang et al., 2014). Thus, deciphering the regulatory mechanisms of IL-1 β production in TB infection is critical for understanding TB pathology and immune responses.

The production of IL-1 β with bioactivity, a tightly regulated process, progresses in two steps. The first step is the expression of inactive pro-IL-1 β by the cells in response to various PAMPs and damage-associated molecular patterns (DAMPs). The second step is the maturation of pro-IL-1 β into an active IL-1 β through its cleavage by activated caspase-1. The activation of caspase-1 is mediated by inflammasome, a multiprotein complex formed in the cytosols of the cells with the involvement of members of NLRP family including NLRP1, NLRP3, and NLRC4 and the adaptor ASC (Martinon and Tschopp, 2007).

The NLRP3-containing inflammasome can be activated by *Mtb* infection in an early secreted antigenic target (ESAT)-6 dependent manner (Mishra et al., 2010), but the mechanisms remain poorly understood.

Although IL-1 β production has been studied extensively, the significance of epigenetic regulatory mechanisms in IL-1 β production remains unclear. In the present study, we demonstrated that inhibition of HDAC2 by chemical and genetic approaches promotes the secretion of mature IL-1 β through the enhanced expression and activation of NLRP3 by primary macrophages and dendritic upon *in vitro* stimulation and *Mtb* infection and in mouse lungs in a low-dose aerosol *Mtb* infection model. Thus, we describe a mechanism of IL-1 β regulation controlled by epigenetic effector molecule, HDAC2, with a significance in TB infection and other chronic inflammatory diseases.

RESULTS

Inhibition of HDAC1 by DHOB markedly increases IL-1 β production by dendritic cells following LPS/CD40LT stimulation

To determine the functional significance of HDACs in IL-1 β production by innate immune cells, we screened 11 zinc-dependent HDACs using chemical inhibitors, such as, Mocetinostat targeting HDAC1, 2, 3, and 11; BRD73954 for HDAC6 and 8; TMP195 for HDAC4, 5, 7, and 9 and Trichostatin A (TSA), a pan-HDAC inhibitor at different concentrations based on the published studies. Our results (Figure 1A) demonstrated that stimulation of human MDDC with LPS plus CD40LT (LPS/CD40LT) induced secretion of IL-1 β compared with the control cells without stimulation, although at relatively low level as reported previously (Wang et al., 2012). To our surprise, out of four different chemical inhibitors targeting 11 HDACs, only Mocetinostat targeting class I HDACs significantly increased LPS/CD40LT-stimulated IL-1 β secretion by MDDC dose dependently compared with the cells stimulated in the presence of DMSO or other HDAC inhibitors. The pan-HDAC inhibitor TSA at all three concentrations did not show any effects on IL-1 β production by MDDC (Figure 1A). In contrast, LPS/CD40LT induced significantly increased levels of other two major inflammatory cytokines TNF- α (Figure 1B) and IL-6 (Figure 1C) compared with the unstimulated control cells, and none of the inhibitors affected the production of these two cytokines. These results indicated that only HDACs 1, 2, 3, and 11 may regulate the production of IL-1 β by DCs. To narrow this list down, we probed the individual members of class I HDACs except for HDAC11 due to lack of specific inhibitor, using MS-275 for targeting HDAC1 and HDAC3, DHOB for HDAC1, and RGFP966 for HDAC3. Our results (Figure 1D) demonstrated that MS-275 and DHOB significantly increased LPS/CD40LT-stimulated IL-1 β production by MDDC dose dependently compared with DMSO control cells. In contrast, RGFP966 did not affect IL-1 β at all three concentrations, suggesting that HDAC1 is the main HDAC regulating IL-1 β production by DC. Similarly, these inhibitors did not affect the production of

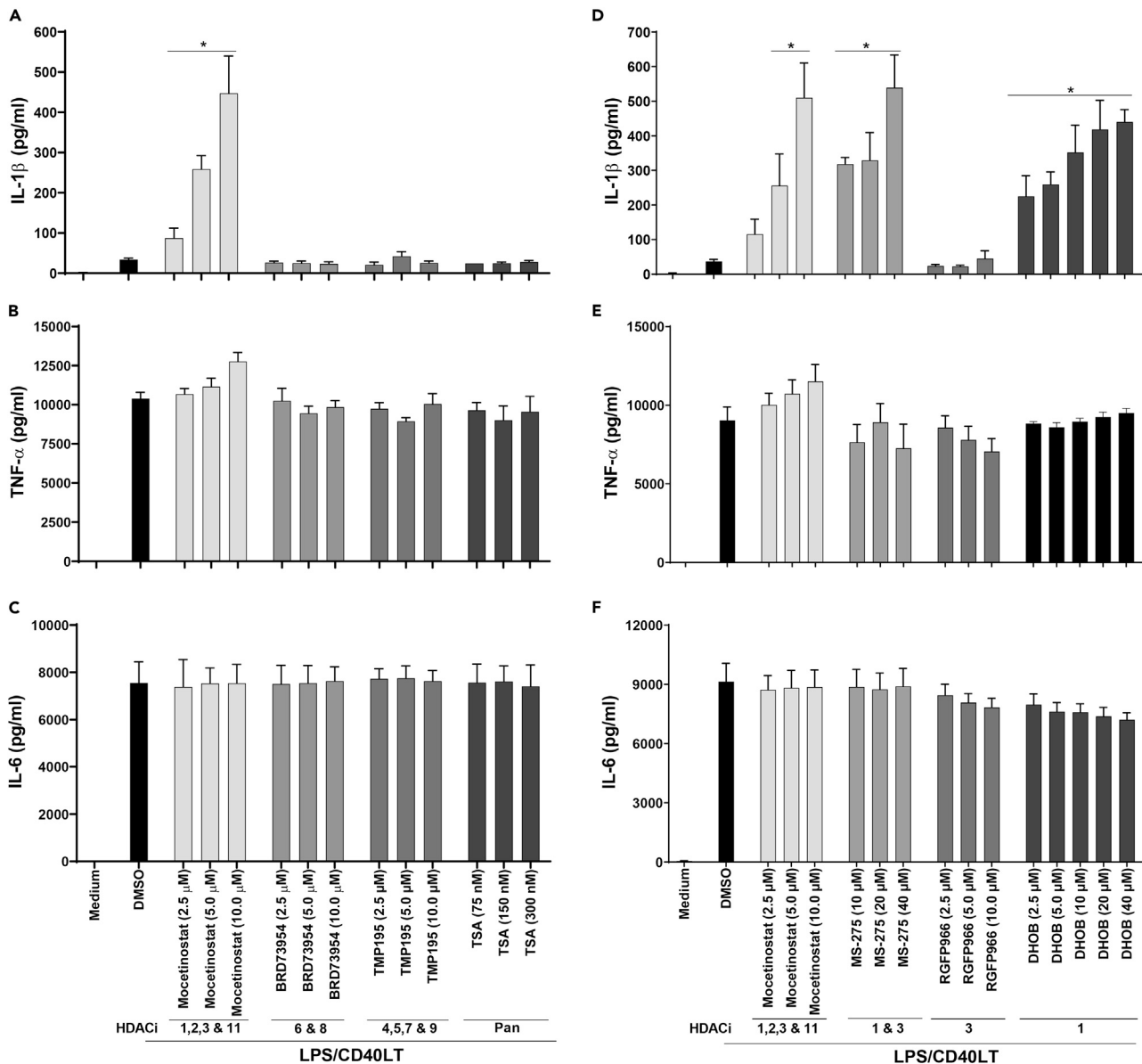


Figure 1. Screening with HDAC inhibitors identifies HDAC1 as a major regulator of IL-1β production

MDDC from four healthy donors were pretreated with the HDAC inhibitors (HDACi) targeting different HDAC isoforms at different concentrations as indicated for 1 h before stimulation with LPS/CD40LT for 16 h. The levels of IL-1β (A and D), TNF-α (B and E), and IL-6 (C and F) in the cell culture supernatants were determined by ELISA. Mean ± SEM are shown. *, $p < 0.05$ compared with DMSO control.

TNF-α (Figure 1E) and IL-6 (Figure 1F) produced by LPS/CD40LT-stimulated DCs. This specific effect of the inhibitors on IL-1β production is not due to cellular toxicity of the inhibitors (Figure S1). These results together suggest that HDAC1 targeted by DHOB is the main HDAC isoform with IL-1β-specific regulatory activity in innate immune cells.

Inhibition of HDAC1 induces maturation and release of IL-1β from *Mtb*-infected dendritic cells

After identifying HDAC1 as the main regulator of IL-1β production by DC in response to LPS/CD40LT stimulation, we examined this in innate immune cells infected with *Mtb*. Before testing this, we determined the capacities of LPS, CD40LT, *Mtb* infection separately or combination of *Mtb* infection with LPS, CD40LT, or LPS/CD40LT stimulation in IL-1β production by DC. Our results showed that although LPS, CD40LT, or

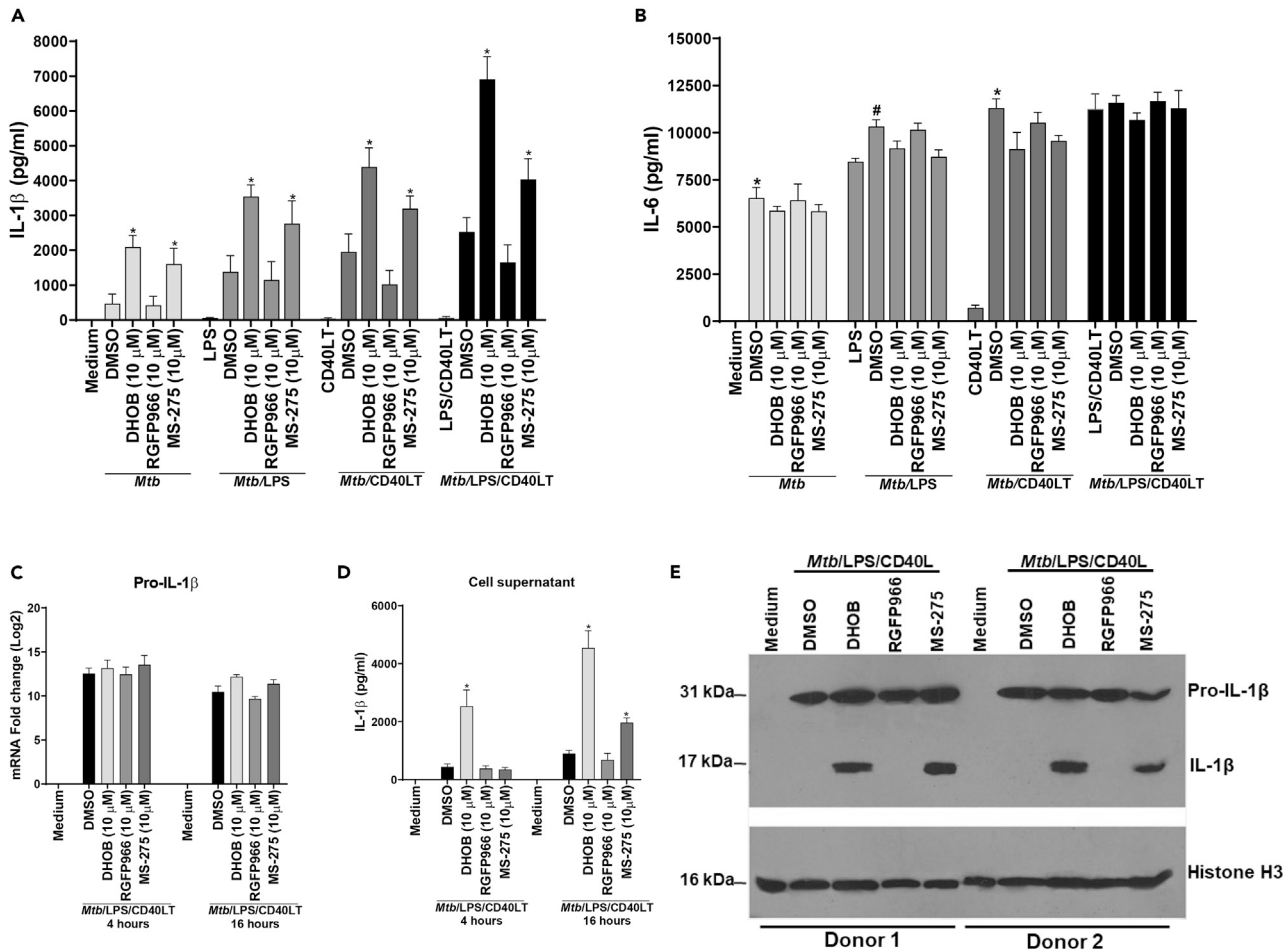


Figure 2. DHOB markedly increases the production of mature IL-1β by DC and macrophages upon *Mtb* infection without affecting mRNA and pro-IL-1β

MDDC from five healthy subjects were either mock infected (Medium) or infected with H37Rv at 5 MOI for 3 h. The infected cells were then treated with DHOB, RGFP966, or MS-275 for 1 h followed by stimulation with LPS, CD40LT, or LPS/CD40LT as indicated for 16 h. The levels of IL-1β (A) and IL-6 (B) in the cell culture supernatants were determined by ELISA. Human MDDC were infected with *Mtb* followed by stimulation with LPS/CD40LT and treatment as in (A), and the levels of IL-1β mRNA (C) in total cell RNA and the protein in the cell culture supernatants (D) were quantified by real-time PCR and ELISA, respectively. Total cell protein extracts of the MDDC infected with *Mtb* followed by stimulation with LPS/CD40LT and treated as in (A) were used for determination of IL-1β protein expression by western blotting. The same nitrocellulose membrane was stripped and reprobed for H3 as a loading control (E). For (E), a representative western blot of four independent experiments is shown. For A–D, mean ± SEM are shown. *, p < 0.05 compared with medium; #, p < 0.05 compared with DMSO control or each group; &, p < 0.05 compared with *Mtb*/DMSO control.

LPS/CD40LT was less potent than *Mtb* infection in stimulation of IL-1β production by DC, combination of *Mtb* infection with LPS, CD40LT, or LPS/CD40LT significantly increased the production of IL-1β by DC, and *Mtb* infection together with LPS/CD40LT stimulation showed as the most potent stimulator of IL-1β production by DC (Figures S2 and 2A DMSO controls). Thus, we have used this combination of *Mtb* infection plus LPS/CD40LT stimulation to test the functional significance of HDACs. Interestingly, inhibition of HDAC1 with DHOB or HDAC1 and 3 with MS-275 significantly increased the production of IL-1β by DC compared with DMSO control cells with *Mtb* infection, *Mtb*/LPS, *Mtb*/CD40LT, or *Mtb*/LPS/CD40LT. In contrast, inhibition of HDAC3 with RGFP966 did not affect IL-1β production (Figure 2A). Consistent with LPS/CD40LT-stimulated DC, these inhibitors did not induce increased production of IL-6 by DC in response to *Mtb* infection, although addition of LPS, CD40LT, or both further increased the production of IL-6 at certain levels (Figure 2B), suggesting that HDAC1 plays critical role in regulating IL-1β production, but not IL-6, by DC infected with *Mtb*.

Because the production of IL-1β is regulated at transcriptional, translational, and post-transcriptional levels and HDACs are known to regulate gene transcription by deacetylation of core histones of the chromatin, we first

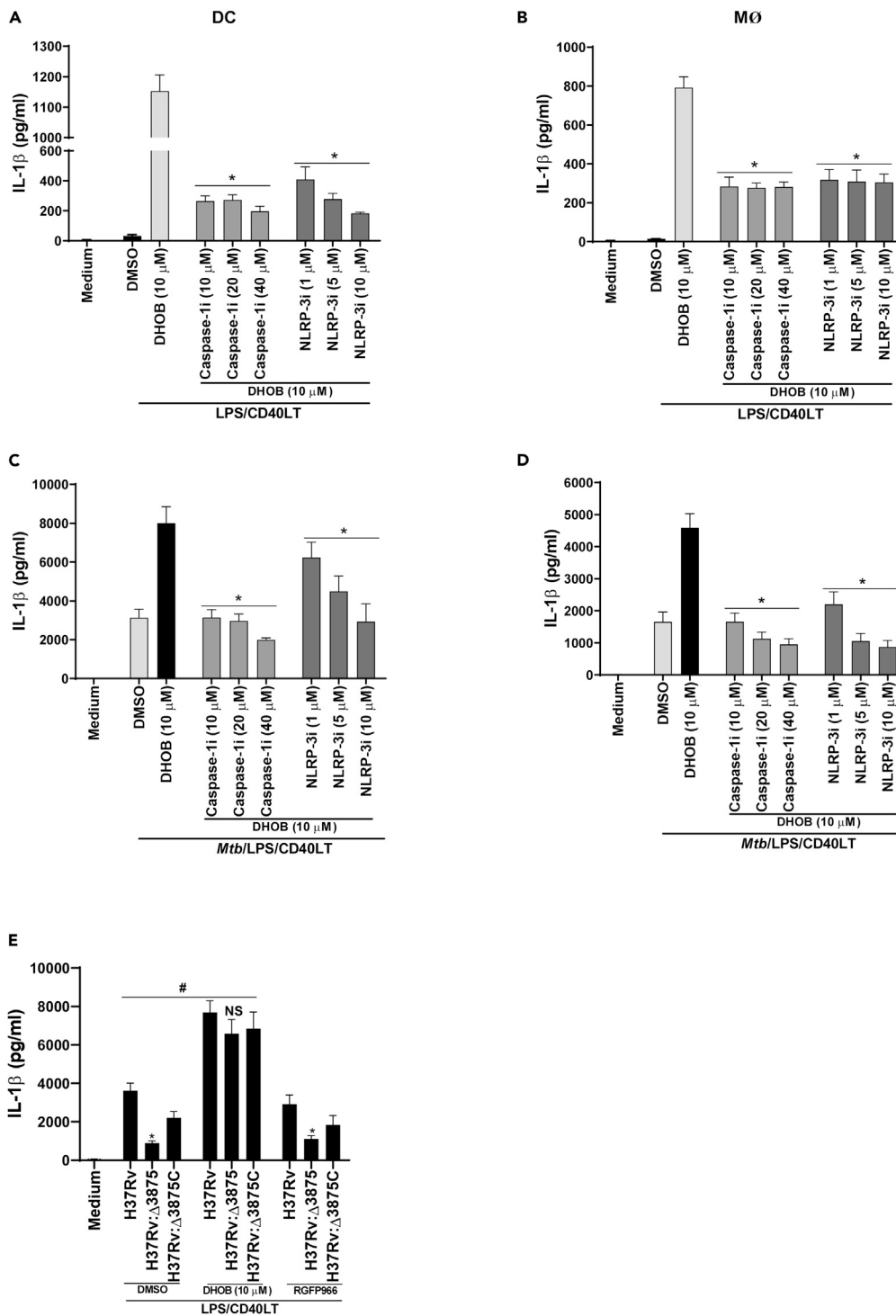


Figure 3. Inhibition of caspase-1 or NLRP3 reverses the enhanced IL-1 β production by DHOB

Human MDDC and MDM from six healthy donors were treated with DMSO or caspase-1 inhibitor II (Caspase-1i) or NLRP3 inhibitor MCC950 (NLRP3i) at indicated concentrations for 1 h and DHOB for another hour before stimulation with LPS/CD40LT (A and B) or infected with H37Rv at 5 MOI for 3 h followed by treatment with the inhibitors as in (A) and (B) before further stimulation with LPS/CD40LT (C and D) for 16 h. MDDC from six healthy donors were infected with H37Rv, its *esat-6* deletion mutant (H37Rv: Δ 3875), or its *esat-6* complemented strain (H37Rv: Δ 3875C) at 5 MOI for 3 h followed by treatment with DMSO, DHOB, or RGF966 for 1 h before stimulation with LPS/CD40LT for 16 h. IL-1 β levels in the culture

Figure 3. Continued

supernatants were determined by ELISA. For all the panels, some cells were incubated without any treatments and infection as controls (medium). Mean \pm SEM are shown. *, $p < 0.05$ compared with wild-type H37Rv; #, $p < 0.05$ compared with DHOB-treated cells; NS, not significant.

tested whether inhibition of HDAC1 affected the transcription of IL-1 β by DC upon *Mtb* infection by treating H37Rv-infected DC with the inhibitors for 1 h before further stimulation with LPS/CD40LT and quantifying IL-1 β mRNA by real-time PCR at 4 and 16 h poststimulation. Compared with the control cells, DC infected with *Mtb* and stimulated with LPS/CD40LT expressed significantly increased IL-1 β mRNA at both time points, and this was not affected by all three inhibitors (Figure 2C) despite DHOB targeting HDAC1 remained effective in increasing IL-1 β production time dependently (Figure 2D). We then determined the effects of these inhibitors on pro-IL-1 β protein levels. Our results demonstrated that *Mtb*-infected DC stimulated with LPS/CD40LT expressed significantly increased pro-IL-1 β compared with the control cells without infection and stimulation, and all three inhibitors did not show any effects on the expression of pro-IL-1 β , although DHOB induced increased the conversion of pro-IL-1 β (31 kDa) into cleaved mature IL-1 β (17 kDa) (Figure 2E); this is not due to differences in samples loading, as reprobing the same nitrocellulose membrane with anti-histone (H)3 Ab after stripping showed comparable levels of H3 across the lanes regardless of the treatment conditions. These results implied that the inhibition of HDAC1 may lead to increased IL-1 β production by targeting the posttranslational maturation process of IL-1 β in innate immune cells.

Inhibition of HDAC1 enhances IL-1 β maturation through the regulation of NLRP3 and caspase-1 activities

The posttranslational regulation of IL-1 β is mediated by cleavage of pro-IL-1 β by caspase-1, the effector molecule of tripartite inflammasome complex that also contains the sensor molecule, NLRP3, and an adaptor molecule, ASC, in response to inflammatory stimulation (Swanson et al., 2019). Thus, we tested whether DHOB enhances IL-1 β maturation and production through NLRP3-mediated caspase-1 activation in our macrophage and DC either stimulated with LPS/CD40LT or *Mtb* infection together with LPS/CD40LT stimulation models by applying proven inhibitors of NLRP3 (CP-456773/MCC 950) and caspase-1 (caspase-1 Inhibitor II). As shown earlier (Figures 2A and S2), the infection of both cell types with H37Rv induced significantly higher amounts of IL-1 β than that of LPS/CD40LT stimulation, and the combination of the infection and stimulation further increased the production of IL-1 β by both cell types, with MDDC producing significantly higher levels of IL-1 β (Figure 3A versus 3C) than that of MDM (Figures 3B and 3D). Interestingly, inhibition of either caspase-1 or NLRP3 reduced DHOB-induced increased production of IL-1 β in both cell types treated with both conditions to the levels of the cells treated with DMSO and stimulated with LPS/CD40LT (Figures 3A and 3B) or H37Rv infection plus LPS/CD40LT stimulation (Figures 3C and 3D). This effect is not due to compromised cell viability due to general cytotoxicity of the chemical inhibitors as determined by MTT assay (Figures S3A and S3B), implying that HDAC1 controls IL-1 β maturation in both cell types through enhanced activities of NLRP3 inflammasome and caspase-1 activation. To confirm this further, we took the advantage of an *esat-6* deletion mutant of H37Rv, which is incapable of inducing mature IL-1 β production by the infected macrophages due to lack of NLRP3 activation compared with its *esat-6* intact wild-type strain, as ESAT-6 secreted by *Mtb* is a potent activator of the NLRP3-inflammasome and caspase-1 activation (Mishra et al., 2010; Wang et al., 2012). Therefore, we assessed whether DHOB can rescue this defect. Consistent with the previous reports (Jung et al., 2021), H37Rv: Δ 3875 was unable to induce IL-1 β production by DC compared with H37Rv or its *esat-6*-complemented strain H37Rv: Δ 3875C, and DHOB significantly increased the production of IL-1 β by DC infected with all three strains of *Mtb* to the comparable levels rescuing compromised IL-1 β production by H37Rv: Δ 3875-infected DC. In contrast, HDAC3 inhibitor, RGFP966, -treated DC infected with H37Rv: Δ 3875 remained low in IL-1 β production as with DMSO control (Figure 3E). These findings together suggest that DHOB enhances IL-1 β production by innate immune cells through NLRP3 and caspase-1.

Because NLRP3 is the rate-limiting factor of IL-1 β maturation (Bauernfeind et al., 2009), we determined the effects of HDAC inhibitors on NLRP3 mRNA and protein expression. The infection of DC with H37Rv and stimulation with LPS/CD40LT induced significantly elevated expression of NLRP3 mRNA compared with the control cells at 4 h poststimulation, and this was maintained until 16 h postinfection. Inhibition of HDAC1, but not HDAC3, significantly elevated the mRNA of NLRP3 compared with the cells with DMSO control at 4-h poststimulation, and this effect was faded by 16 h poststimulation (Figure 4A). At the protein level, infection of MDDC and MDM with H37Rv and stimulation with LPS/CD40LT increased the protein levels of NLRP3 compared with the control cells and DHOB, but not RGFP966, increased the expression

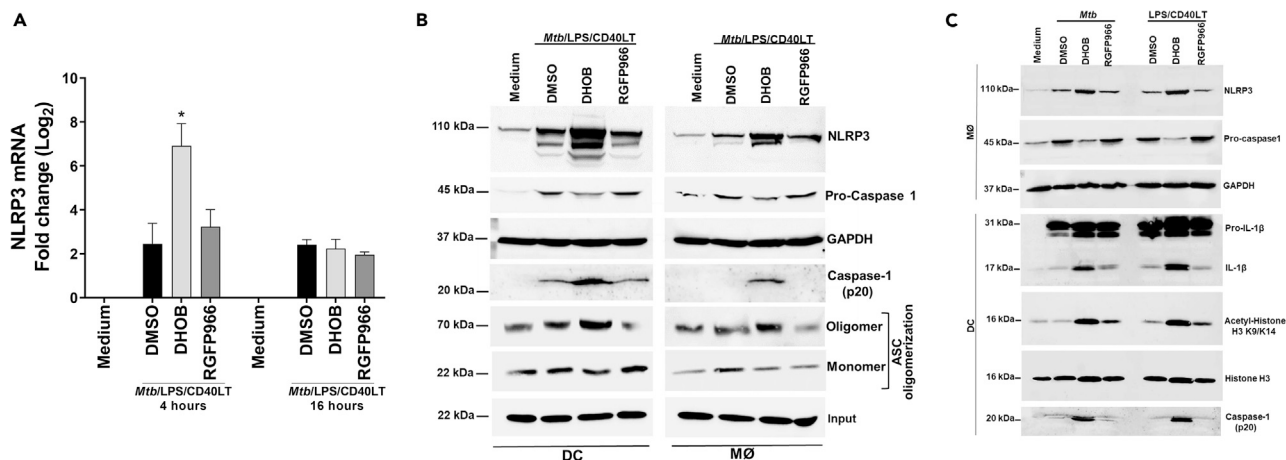


Figure 4. DHOB increases IL-1 β maturation from *Mtb*-infected cells through elevated expression of NLRP3

(A) MDDC from four healthy donors were infected with H37Rv at 5 MOI for 3 h and were treated with DHOB or RGFP966 at 10 μ M or DMSO for 1 h before stimulation with LPS/CD40LT. NLRP3 mRNA in total cell RNA was quantified by real-time PCR at 4- and 16-h poststimulation. (B) MDDC and MDM were treated as in A for 16 h and the protein levels of NLRP3, pro-caspase-1, oligomerization of ASC in protein extracts, and cleaved caspase-1 (p20) in the cell culture supernatants were determined by western blotting. ASC levels in the protein extracts without crosslinking were blotted as an input control for ASC oligomerization assay. The same nitrocellulose membranes were re probed with GAPDH after stripping as loading control. (C) Human MDDC were infected with H37Rv for 3 h followed by treatment with DMSO, DHOB, or RGFP966 at 10 μ M or pretreated with the inhibitors for 1 h before stimulation with LPS/CD40LT for 16 h. The protein levels of NLRP3, acetylated H3K9/K14 in protein extracts, were determined by western blotting using GAPDH for macrophages and H3 for DC as loading controls. For (A), mean \pm SEM are shown. *, $p < 0.05$ compared with H37Rv-infected cells of each group; #, $p < 0.05$ compared with DMSO control. For (B), (C), and (A) one representative result of 4 is shown.

of NLRP3 dramatically compared with the cells with DMSO (Figures 4B and 4C). Pro-caspase 1 (p45) was also increased in the cells with infection and stimulation compared with the control cells, and DHOB, but not RGFP966, elevated the levels of cleaved caspase-1 (p20) in the respective cell culture supernatants, and oligomerization of ASC was increased in the cells upon infection and stimulation, and DHOB significantly increased the oligomerization of ASC (Figures 4B and 4C) without affecting total ASC expression levels (Figure 4B input), indicating the elevated activation of caspase-1 and ASC oligomerization compared with DMSO control cells, consistent with significantly increased IL-1 β production due to increased NLRP3 inflammasome activation upon DHOB treatment. The changes in NLRP3 expression in differentially treated cells are not due to uneven sample loading, as there were same levels of GAPDH detected across the lanes on the same membrane (Figures 4B and 4C).

The acetylation of histone H3K9/K14 of macrophages and DCs correlates with NLRP3 activation in *Mtb*-infected cells following HDAC1 inhibition

Thus far, our results have demonstrated that HDAC1 plays a critical role in *Mtb*-infection-induced production of inflammatory cytokine IL-1 β through the regulation of inflammasome sensor NLRP3 and NLRP3 inflammasome activation in innate immune cells. Because activation of HDAC1 is associated with elevated deacetylase activity for the removal of acetyl group from the lysine residue of histones, we determined the changes in acetylation of H3 at lysine 9 and 14 (H3K9/K14). We observed that both DHOB and RGFP966 increased H3K9/K14 significantly in MDDC infected with *Mtb* or stimulated with LPS/CD40LT compared with the control cells with medium and with DHOB stronger than that of RGFP966 in suppression of H3 deacetylase activity (Figure 4C). Consistent with this result, DHOB and other two inhibitors, MS-275 and Mocetinostat, showed the most potent activities in blocking H3 deacetylase activities followed by RGFP966 and TSA as the lowest. The other two inhibitors, TMP195 and BRD73954, did not show any activity. These were consistent with activation of caspase-1 (Figure S4). These together suggest that Class I HDACs except for HDAC8 play dominant roles in removal of acetyl group from the lysine residue of H3, consistent with recent report showing that HDAC1, 2, and 3 are the most efficient deacetylases *in vitro* (Moreno-Yruela et al., 2022). Interestingly, compared with medium control cells, *Mtb* infection or LPS/CD40LT stimulation reduced the acetylation of H3K9/K14 (Figure 4C), indicating the induction of histone deacetylase activities in innate immune cells by *Mtb* infection and stimulation at certain levels. DHOB promoted the maturation of IL-1 β through NLRP3 expression in response to either *Mtb* infection or LPS/CD40L stimulation, consistent with increased acetylation of H3K9/K14 confirming the effect of DHOB. Interestingly, inhibition of

HDAC3 does not contribute to the maturation and production of IL-1 β by innate immune cells (Figure 4B and 4C), although inhibition of HDAC3 increased acetylation of H3K9/K14 at certain level, which was lower than that of HDAC1 inhibition.

To verify whether new protein synthesis is required for DHOB-induced expression of NLRP3 transcription, DC were treated with cycloheximide, a protein synthesis inhibitor, before treatment with HDAC1 inhibitor and stimulation with LPS/CD40LT. Inhibition of new protein synthesis blocked the effect of DHOB-induced increased expression of NLRP3 mRNA (Figure S5), indicating that new protein synthesis is required for DHOB-enhanced expression of NLRP3 mRNA in innate immune cells.

Mtb infection and stimulation of DC induces activation of HDAC, which was suppressed by DHOB

To corroborate the findings with reduced deacetylation of H3 by HDAC inhibitors with HDAC expression and activation, we examined the expression of HDAC1, 2, and 3 and demonstrated that *Mtb* infection increased expression of HDAC1 and HDAC2, but not HDAC3, although at modest level compared with the cells without infection (Figure 5A). Consistent with this, analysis of publicly available data on mRNA expression of HDAC1 and HDAC2 expression in PBMC of latent tuberculosis-infected (LTBI) subjects and TB patients (Cai et al., 2014) showed increased HDAC1 mRNA expression in TB patients compared with that of LTBI subjects and HDAC2 showed reduced trend, although not significant compared with their LTBI controls (Figure S6). We then performed an HDAC activity assay using total cell protein extracts from H37Rv-infected DC stimulated with LPS/CD40LT. Indeed, the assay demonstrated that *Mtb* infection and stimulation by LPS/CD40LT increased pan-HDAC activity when compared with the cells with medium control, and DHOB induced a robust reduction of this activity that was even lower than that of controls cells and the cells that were treated with RGFP966, implying that the HDAC activity induced by *Mtb* infection and stimulation is contributed mainly by HDAC1 (Figure 5B). We then examined the HDAC1, 2, and 3 specific activities and the effects of HDAC inhibitors by performing HDAC activity assay using immunoprecipitated HDAC1, 2, and 3 from the total protein extracts of MDDC infected with *Mtb* and treated with DHOB as HDAC source for the intracellular effects of DHOB or directly treating HDAC1, 2, and 3 with DHOB in the test tubes after immunoprecipitated from the total cell protein extracts infected with *Mtb* and treated with DMSO. The results showed that HDAC1 and HDAC2, but not HDAC3, were the major contributors to the HDAC activities of DC infected with *Mtb*, and DHOB suppressed deacetylase activities of both HDAC1 and HDAC2, and HDAC3 remained low in HDAC activities (Figure 5C). To our surprise, DHOB completely suppressed the activities of both HDAC1 and HDAC2 but did not affect that of HDAC3 upon direct incubation (Figure 5D). The differential activities of immunoprecipitated HDACs were not due to low immunoprecipitation efficiencies (Figure 5E). These results together suggest that DHOB, although used as an HDAC1 inhibitor (Bauer et al., 2021; Bazou et al., 2016; Moon et al., 2017), targets both HDAC1 and HDAC2.

DHOB interacts with both HDAC1 and HDAC2

We examined whether DHOB binds to HDAC1 and HDAC2 by *in silico* molecular docking studies. Consistent with high homology, HDAC1 and HDAC2 were superimposed on each other structurally, and the docking studies found nine highest scoring (tight DHOB binding) positions for each protein, and this binding can interfere with the active site tunnel as depicted for one such position for both proteins (Figures 6A–6C). This finding supports that DHOB inhibits the activity of both HDAC1 and HDAC2 by direct binding to the active sites of the proteins. To further corroborate this, we performed drug affinity responsive target stability (DART) to test whether DHOB protects HDAC1 and HDAC2 from proteinase digestion as a small molecule binding to their specific ligands (Lomenick et al., 2009). We showed (Figure 6D) that preincubation of cellular protein extracts with DHOB at both concentrations protected HDAC1 and HDAC2 from pronase digestion compared with the proteins preincubated with DMSO control. This protection is specific for HDAC1 and HDAC2 because DHOB did not protect HDAC3 and the pronase did not digest GAPDH differentially because of DHOB when examined for GAPDH, which was relatively resistant to pronase (Pai et al., 2015). These data together support the potential direct binding of DHOB with both HDAC1 and HDAC2 and suppressing their histone deacetylase activities.

Knockdown of HDAC2, but not HDAC1, enhances IL-1 β maturation through the regulation of NLRP3

To determine whether DHOB induces increased secretion of IL-1 β by innate immune cells by targeting HDAC1 or HDAC2, we knocked down HDAC1 or HDAC2 in human macrophage cell line THP1 expressing

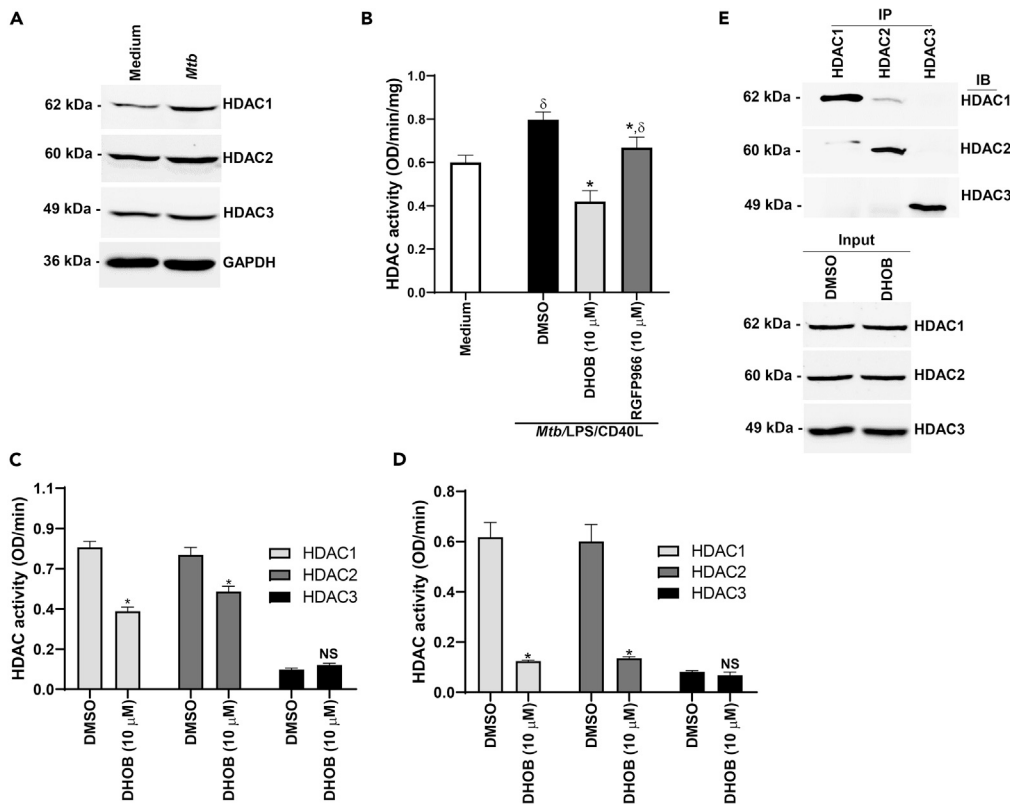


Figure 5. *Mtb* infection or stimulation induces elevated expression and activity of histone deacetylase in macrophages and DC, which is blocked by DHOB

Human MDDC were infected H37Rv at 5 MOI for 16 h, and the expression of HDACs as indicated was determined by western blotting using GAPDH as loading control (A). Human MDDC were infected H37Rv as in (A) for 4 h and incubated with either DHOB or RGFP966 or DMSO as control for 1 h before stimulation with LPS/CD40LT. Some cells were kept as medium control without infection and stimulation. Sixteen hours later, the HDAC activities in protein extracts were determined by pan HDAC activity assay (B). Immunoprecipitated HDAC1, HDAC2, and HDAC3 from the protein extracts of the cells treated as in (B) were assayed for HDAC activity (C). The immunoprecipitated HDACs from the cells infected and stimulated in the presence of DMSO were assayed for HDAC activity in the presence of DMSO or DHOB (D). For the determination of immunoprecipitation efficiencies, the immunoprecipitated HDACs were determined by western blotting (IB). The protein extracts of the cells were used as input control for the immunoprecipitation (E). A representative western blot result of 4 (A) and 3 (E) independent experiments is shown. Mean \pm SEM of four healthy donors with two technical replicates for each sample are shown for (B–D). δ , $p < 0.05$ compared with medium (B); *, $p < 0.05$ compared with DMSO control (C and D); NS, not significant compared with DMSO control.

Cas9 gene using CRISPR/Cas9 gene-editing approach. After confirming the KD of HDAC1 or HDAC2 in comparison to cgRNA-transfected THP-1 cells by western blotting (Figure 7A), the cells were differentiated into macrophages and were infected with H37Rv at 5 MOI for 3 h followed by treatment with DHOB, and the expression of NLRP3 and acetylation of H3K9/K14 in total cell protein extracts and IL-1 β in culture supernatants were determined by western blotting and ELISA, respectively, at 16 h postinfection. Consistent with primary human innate immune cells, cgRNA-transfected THP-1-derived macrophages expressed increased NLRP3 upon *Mtb* infection compared with the noninfected control cells, and this was further increased by DHOB. The control macrophages showed reduced acetylation of H3K9/K14 upon *Mtb* infection, and this was increased by DHOB. Macrophages with HDAC1KD behaved similarly as cgRNA-transfected control macrophages in their expression of NLRP3 and acetylation of H3K9/K14. In contrast, macrophages with HDAC2KD expressed increased NLRP3 and acetylated H3K9/K14 even in the cells without infection compared with the cells with cgRNA and HDAC1KD, and this was further increased dramatically upon *Mtb* infection, and the presence of DHOB showed minimal effects. These differences are not due to variable protein loading as similar expression levels of GAPDH and H3 detected across the lanes (Figure 7A). Consistent with changes in protein expression, cgRNA-transfected macrophages and HDAC1KD cells

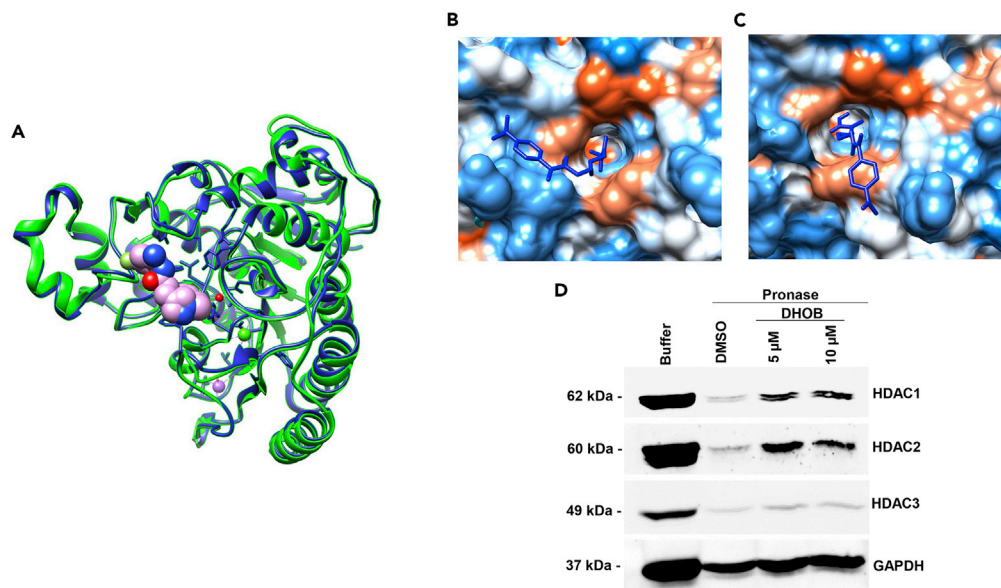


Figure 6. DHOB binds to both HDAC1 and HDAC2 and protects them from proteinase digestion

Comparison of overlapping three-dimensional structures of HDAC1 (blue) and HDAC2 (green) with DHOB (shown as spheres) bound to the same location on both proteins with zinc shown in red (A). Hydrophobic surfaces of HDAC1 (B) and HDAC2 (C) with bound DHOB (blue) showing the binding mode of the DHOB, shown as licorice, interfering with the active site of HDAC1 and HDAC2. Preincubation of cellular protein extracts with DHOB, but not DMSO, protects from pronase digestion (D). For panel (D), one representative result of three different experiments is shown.

produced significantly increased IL-1 β compared with their control cells without infection, and this was further increased significantly by DHOB. In contrast, macrophages with HDAC2KD produced significantly higher IL-1 β production than both cgRNA-transfected cells and HDAC1KD cells without *Mtb* infection, which was further increased significantly by *Mtb* infection, and the presence of DHOB did not further increase the production of IL-1 β (Figure 7B). The similar results were also obtained with the cells stimulated with LPS/CD40LT for IL-1 β production although with visible effects of DHOB (Figure 7C). Because HDAC2 exhibits 85% of total sequence identity with HDAC1 (Grozinger and Schreiber, 2002) as also shown in Figure 6A and DHOB reduced HDAC activities of both HDAC1 and HDAC2, to further confirm this effect of HDAC2, we used BRD6688, a chemical inhibitor of HDAC2 with longer effects in both *in vitro* and *in vivo* models (Aufhauser et al., 2021; Wagner et al., 2015), to test the effect of blocking HDAC2 on IL-1 β production by *Mtb*-infected human MDM. Our results demonstrated that blocking HDAC2 with BRD6688 significantly increased the production of IL-1 β by MDM compared with the cells treated with DMSO control in a concentration-dependent manner, with 0.25–1.0 μ M already showing significantly increased IL-1 β production and gradual reduced effects with 2.5–5.0 μ M concentration (Figure 7D). Nonetheless, these results together demonstrated that HDAC2, but not HDAC1, enhances IL-1 β maturation and secretion through the increased NLRP3 inflammasome activation.

DHOB enhances IL-1 β production in a mouse model of *Mtb* infection

To confirm whether the findings from *in vitro* studies with primary human innate immune cells are applicable to mouse cells and confirm the findings with a live *Mtb* infection model, we investigated the effect of DHOB on IL-1 β production by mouse innate immune cells. Consistent with the findings from human immune cells, stimulation of BMDD with LPS/interferon gamma (IFN- γ) induced significantly elevated production of IL-1 β and DHOB increased IL-1 β production significantly compared with the cells stimulated in the presence of DMSO (Figure 8A). Infection of BMDD or BMDM with H37Rv also induced significantly increased IL-1 β production in a dose-dependent manner and DHOB, but not RGFP966, further elevated IL-1 β production significantly compared with the infected cells treated with DMSO (Figures 8B and 8C). Consistently, the cells stimulated in the presence of DHOB, but not RGFP966, increased the levels of mature IL-1 β in the culture supernatants when determined by western blotting (Figures 8D and 8E).

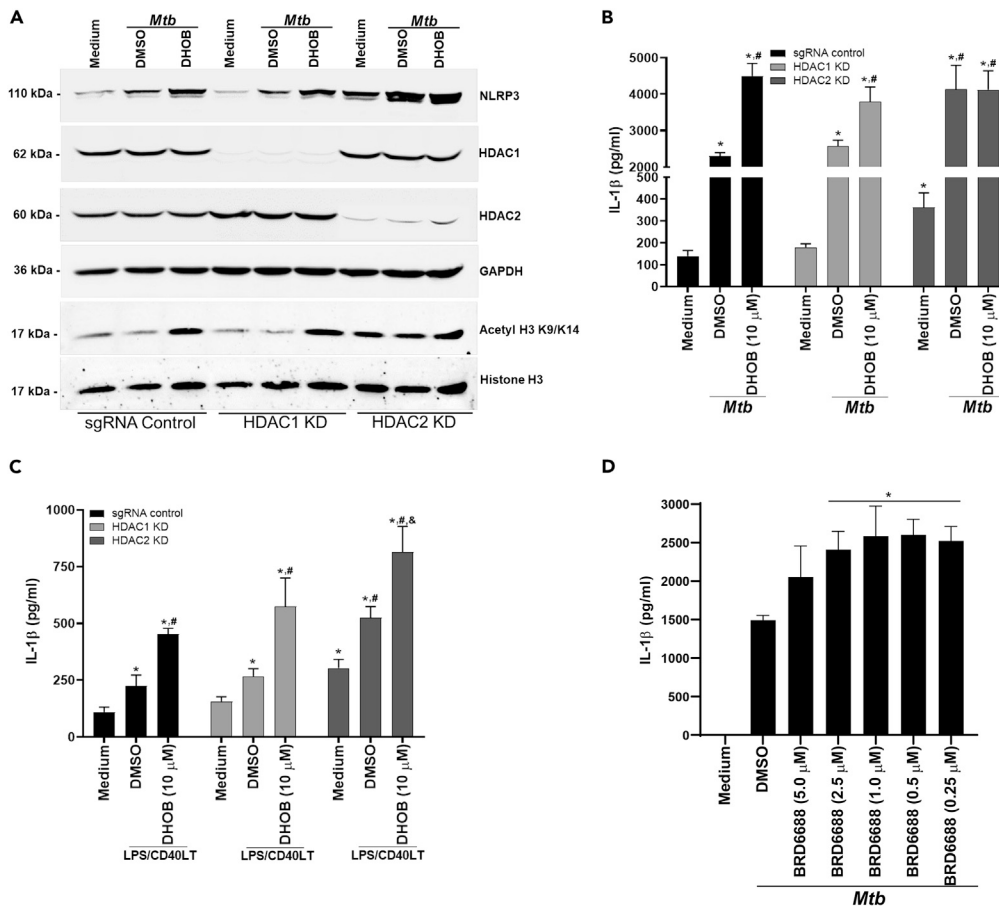


Figure 7. Knockdown of HDAC2, but not of HDAC1, increases IL-1 β maturation from *Mtb*-infected cells through elevated expression of NLRP3 and acetylation of H3K9K14

(A) The macrophages derived from THP-1 cells transfected with control sgRNA or CRISPR-Cas9 knocked down (KD) of HDAC1 or HDAC2 were infected with H37Rv at 5 MOI for 3 h before incubation with DHOB at 10 μ M or DMSO for 1 h. The cells were incubated overnight and the expression of NLRP3, HDAC1, HDAC2, and acetylated H3K9K14 in proteins extracts were detected by western blots. The membranes were stripped and reprobed for GAPDH and H3 as loading controls (A). The IL-1 β levels in the cell culture supernatants of the cells treated as in (A) were determined by ELISA (B). The same cells were pretreated with either DHOB or DMSO as in (A) for 1 h before stimulation with LPS/CD40LT. IL-1 β in the cell culture supernatants at 16 h post-stimulation was determined by ELISA (C). Human MDM from five healthy donors were infected with H37Rv as in (A) and treated with either DMSO or BRD6688 at indicated concentrations. Sixteen hours later, IL-1 β levels in the cell culture supernatants were determined by ELISA. A representative western blot of four independent experiments is shown in (A). Mean \pm SEM are shown in (B–D). *, $p < 0.05$ compared with DMSO control; *, #, $p < 0.005$ compared with the cells with DMSO; *, #, &, $p < 0.0005$ compared with the cells with DMSO.

We then treated low-dose aerosol H37Rv-infected C57BL/6 mice with DHOB or DMSO as vehicle control by IP injection. Our results from two-week infection model to avoid the confounding effects of adaptive immunity on IL-1 β production demonstrated that DHOB treatment resulted in significantly increased IL-1 β production in the mouse lungs compared with that of the mice treated with DMSO (Figure 8F). Consistently, DHOB did not affect the production of IL-6 (Figure 8G). DHOB treatment also increased mRNA expression of NLRP3 in the mouse lung significantly higher than that of the mice treated with DMSO (Figure 8H), supporting the *in vivo* significance of DHOB in regulation of IL-1 β in *Mtb* infection.

DISCUSSION

IL-1 β plays critical roles in both protection against and pathology of the intracellular bacterial infections including *Mtb* infection and the development of chronic inflammatory diseases including autoimmune diseases. Therefore, it has been the focus of extensive research to understand the molecular mechanisms of

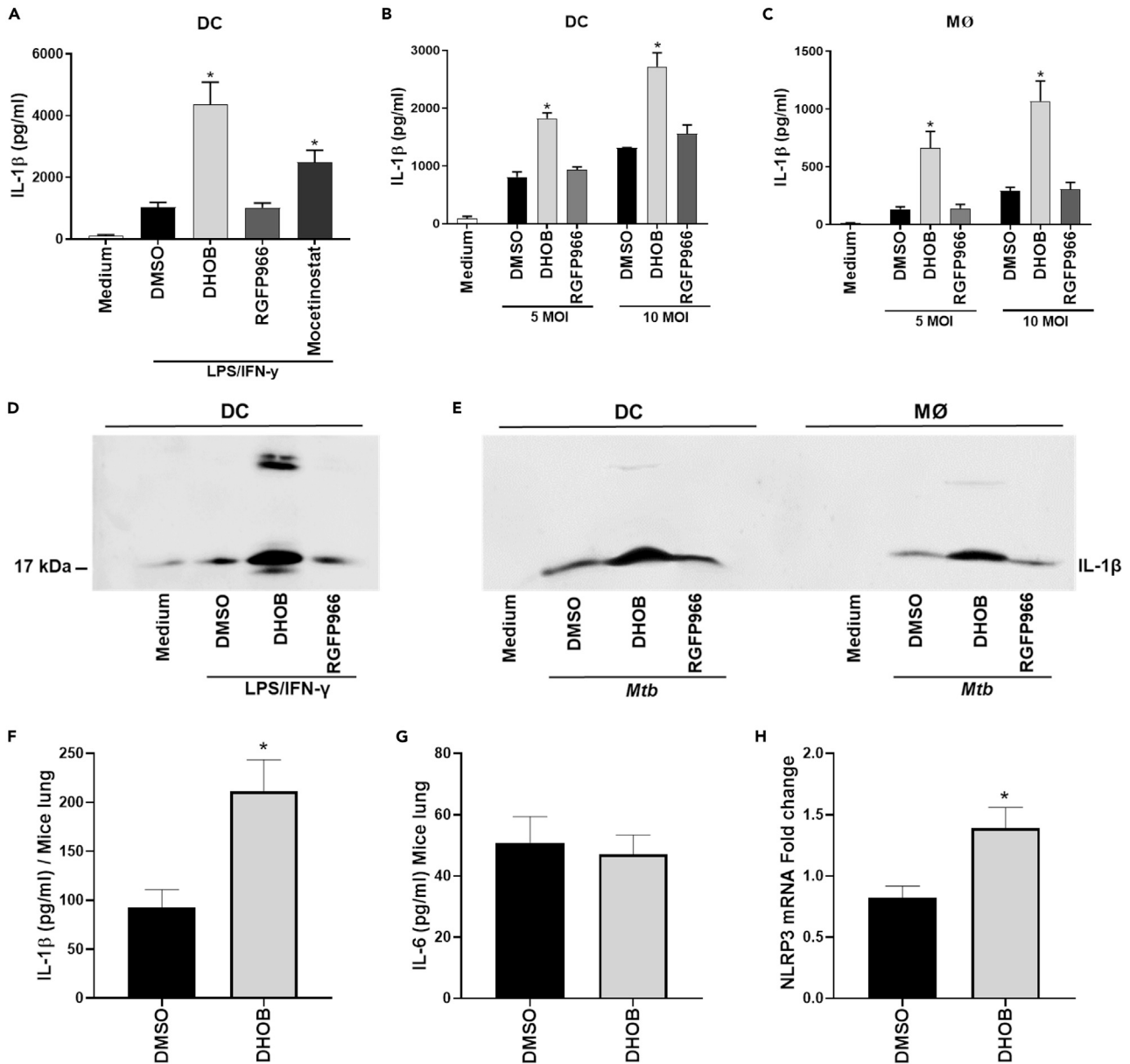


Figure 8. DHOB increases IL-1 β production both *in vitro* and *in vivo* *Mtb* infection models

Mouse BMDD were pretreated with DHOB, RGFP966, or Mocetinostat at 10 μ M or DMSO as control for 1 h before stimulation with LPS/IFN- γ for 16 h. The IL-1 β levels (A) and cleaved IL-1 β (D) in the cell culture supernatants were determined by ELISA and western blotting, respectively. Mouse BMDD or BMDM infected with H37Rv at 5 and 10 MOI for 3 h were treated with indicated inhibitors for 1 h followed by stimulation as in (A), and the production of IL-1 β and cleaved IL-1 β in the cell culture supernatants were determined by ELISA (B and C) and western blotting (E), respectively. Mice were infected with H37Rv and treated by IP injection of DHOB or DMSO control daily for 6 days a week for 2 weeks. At the end of the treatment, the lung homogenates were evaluated for IL-1 β (F) and IL-6 (G) by ELISA, and NLRP3 mRNA expression (H) in total lung RNAs was quantified by real-time PCR using GAPDH as internal control and expressed as fold change over that of noninfected control mice. The data are expressed as mean \pm SEM of four mice of each group of one representative experiment of two independent experiments. *, $p < 0.05$ compared with DMSO control. For protein expression analysis, a representative image of three independent experiments is shown. *, $p < 0.05$ compared with DMSO control.

biologically active IL-1 β production, and the studies have uncovered major pathways of its expression, cleavage, and secretion by innate immune cells. Our studies with both chemical-inhibitor-based screening and CRISPR-Cas9-based genetic studies with primary innate immune cells *in vitro* and live animal-based models demonstrated that epigenetic effector molecule HDAC2 plays critical roles in regulation of bioactive IL-1 β production by innate immune cells through the regulation of NLRP3 inflammasome activation by

increased expression and activation of NLRP3, a rate-limiting factor of IL-1 β production by innate immune cells.

It was shown previously that SAHA, sodium butyrate, and TSA, pan-HDAC inhibitors, increase IL-1 β production, respectively, in human macrophages and monocytes upon *Mtb* infection (Cox et al., 2020; Seshadri et al., 2017; Stammler et al., 2015). It was also shown that depsipeptide, a potent HDAC1 and HDAC2 inhibitor, induces a slight increase in IL-1 β by monocytes following *Mtb* infection (Seshadri et al., 2017). However, the molecular details of which and how HDACs regulate IL-1 β remain unexplored.

In the present study, by screening 11 zinc-dependent HDAC variants we identified that class I HDAC, except for HDAC8, are critical in regulation of IL-1 β secretion by innate immune cells. By application of more specific inhibitors of class I HDACs, we found that DHOB previously used as HDAC1 inhibitor (Bauer et al., 2021; Bazou et al., 2016; Moon et al., 2017) promotes the secretion of mature IL-1 β *in vitro* by both human and mouse primary macrophages and DC and human cell lines in response to TLR4 stimulation and *Mtb* infection. However, based on molecular docking, DARTS and histone deacetylase activity analysis further revealed that DHOB has the potential to bind and inhibit both HDAC1 and HDAC2 deacetylase activities consistent with their shared high degree (>80%) of homology in amino acid sequences. Furthermore, CRISPR-Cas9 gene editing showed that knockdown of HDAC2, but not HDAC1, promotes IL-1 β secretion through the posttranslational maturation process of IL-1 β , indicating a separation of their function in IL-1 β regulation by the two highly homologous HDAC despite shown to be redundant in several functions due to their high homology (Gregoretto et al., 2004) and co-expression, and even exists as heterodimers as part of the repressor complexes (Kim et al., 2020; Liu et al., 2020). Three lines of evidence support this conclusion. First, the inhibition of NLRP3 or caspase-1, the sensor or effector molecules of active NLRP3 inflammasome, reversed the elevated levels of IL-1 β induced by DHOB to the comparable levels with the DMSO control cells. Second, DHOB increased the expression of NLRP3 at both mRNA and protein levels; this was further supported by the reduction of pro-caspase-1 (45 kDa) and correspondingly increased active form of cleaved caspase-1 in the culture supernatants of human macrophages and DC exposed to DHOB (Figure S4), suggesting that HDAC2 regulates IL-1 β maturation indirectly at least in part by regulation of NLRP3 expression and activation, caspase-1 activation, and ASC oligomerization to form active NLRP3 inflammasome. Lastly, the previous studies have shown that *Mtb* infection of macrophages induces the production of mature IL-1 β in an ESAT-6-dependent manner, and the secretion of ESAT-6 is associated with and may directly activate NLRP3 for the maturation and secretion of IL-1 β (Mishra et al., 2010; Wang et al., 2012; Jung et al., 2021). Consistent with these observations, our results demonstrated that DHOB restored the release of IL-1 β by DCs infected with *Mtb* lacking *esat-6*. These results implicate that HDAC2 is a major regulator of NLRP3-mediated activation of caspase-1 and ASC oligomerization, a rate-limiting factor of mature IL-1 β production. However, how blocking HDAC2 resulted in increased NLRP3 expression and activation remain to be explored in the future studies with a focus on transcriptional regulators of NLRP3 with acetylation modifications.

In addition, we have also provided an *in vivo* evidence for the significance of HDAC2 inhibition in TB infection despite the complications of HDACs expressed by many different cell populations including both immune cells as well as nonmyeloid cells (Thiagalingam et al., 2003). Treatment of *Mtb*-infected mice with DHOB for two weeks postinfection increased IL-1 β and mRNA expression of NLRP3 without affecting IL-6 production in mouse lung tissues. As a proof of concept, we performed two-week *Mtb* infection model to study the effect of DHOB on production of IL-1 β by innate immune cells without the complications of immune regulation imposed by the adaptive immune responses such as IFN- γ produced by Th1 cells may suppress the production of IL-1 β through iNOS and NO production (Mayer-Barber et al., 2011; Mishra et al., 2013). Because the pathological effects of IL-1 β is evident in chronic TB infection, the role of HDAC2-mediated regulation of IL-1 β production in chronic TB infection in mouse models may provide in-depth understanding of the significance of the HDAC2 in TB infection in terms of IL-1 β regulation, and this can be addressed in the future studies.

The levels of IL-1 β production are often associated with the severity of TB infection (Tsao et al., 1999; Zhang et al., 2014), and blocking IL-1 β activity with a Food and Drug Administration (FDA)-approved drug, anakinra, an IL-1 β receptor blocker, in a mouse model and a nonhuman primate model of TB infection improved the therapeutic outcomes of otherwise toxic linezolid treatment of TB infection due to increased IL-1 β production (Winchell et al., 2020). The production of IL-1 β in response to *Mtb* is dependent on the NLRP3-inflammasome/caspase-1 pathway. However, it was reported that cleaved mature IL-1 β is found

in lungs of *Mtb*-infected mice even in the absence of the NLRP3 or caspase-1 and did not result in different bacterial burdens in lungs and spleen (McElvania Tekippe et al., 2010; Walter et al., 2010), and the lung lesions induced by *Mtb* infection were not affected by the absence of NLRP3 (Dorhoi et al., 2012; McElvania Tekippe et al., 2010; Walter et al., 2010). Thus, understanding the mechanisms of IL-1 β production and associated inflammasome activation pathways in TB infection may provide insights into the mechanisms regulating the secretion of IL-1 β , a key mediator of inflammation and immunity in TB infection, and other bacterial infections and chronic inflammatory diseases.

Accumulating evidence indicates that epigenetic mechanisms participate in the modulation of inflammasomes expression during infection (Liu et al., 2018; Sahu and Sahu, 2015; Wei et al., 2016). It was showed that macrophages infected by *Leishmania amazonensis* dampens NLRP3 inflammasome activation and leads to reduced IL-1 β secretion that correlates with H3K9/K14 hypoacetylation (Lecoeur et al., 2020). Our findings demonstrated a strong increase of acetylation of H3K9/K14 in cells following deletion of HDAC2 compared with the wild-type THP-1 macrophages. Interestingly, we also noticed increased acetylation of H3K9/14 in the cells treated with HDAC3 inhibitor under both *Mtb* infection and LPS/CD40LT stimulation, although at a lower extent than that of the cells treated with DHOB (Figure S4) and no significant difference observed in HDAC1 KD cells compared with wild-type THP-1 macrophages, indicating that HDAC2 is probably the dominant HDAC isoform that deacetylates H3K9/K14 and other nonhistone proteins with lysines. Indeed, the HDAC activity assay demonstrated that infection of DC with *Mtb* and stimulation with LPS/CD40LT induced activation of HDAC and that inhibition of HDAC2 by DHOB led to a robust reduction of HDAC activity induced by *Mtb* infection, further indicating that HDAC2 is the dominant HDAC isoforms in both human and mouse macrophages and DC. Although several other HDACs such as HDAC3 (Angiolilli et al., 2017), HDAC8 (Li et al., 2015), and probably HDAC11 (Stammler et al., 2015) were shown to involve in regulation of inflammatory cytokines, our study was not able to show the effects of these HDACs in regulation of IL-1 β and the chemical inhibitor, and gene-editing studies showed that HDAC2 is the only HDAC isoform with the significant effects on IL-1 β production without affecting IL-6 and TNF- α . This discrepancy may be due to the experimental model, as we used *Mtb* infection and LPS/CD40LT stimulation and differences in cell preparation and differentiation as Angiolilli et al. used GM-CSF-differentiated mouse BMDD instead of GM-CSF plus IL-4 as we did, Li et al. used human PBMC stimulated with LPS, not purified myeloid cells, and Stammler et al. used fibroblast-like synoviocytes isolated from synovial tissues of rheumatoid arthritis patients stimulated with cytokines IL-1 β and type I interferon.

Acetylation of lysine residues at the N-terminal histone tails is tightly controlled by opposing activities of histone acetyl transferases (HATs) and HDACs. It has been identified recently that Rv3423.1 is a histone acetyltransferase secreted by virulent *Mtb* and acetylates H3K9/K14 (Jose et al., 2016). Therefore, HDAC2 may act to counterbalance the acetylation of H3K9/K14 induced by *Mtb* infection, suggesting a potential role for HDAC2 in regulation of immune responses against *Mtb* infection besides regulating IL-1 β production. Our findings demonstrated that the inhibition of HDAC2 also increased NLRP3 expression and IL-1 β secretion in cells stimulated with LPS/CD40LT (Figure S4). Thus, it seems likely that HDAC2 exerts a protective effect against excessive inflammatory response through innate immune cells and can be extended to other chronic inflammatory diseases such as TB infection.

Therefore, it is tempting to speculate that some degree of deficiency in HDAC2 expression or activity in immune cells, especially in macrophages and DC, may associate with overactive inflammation and tissue damage in TB infection. This mechanism may also play a role in chronic inflammatory diseases, such as autoimmune diseases. Indeed, it has been demonstrated that the HDAC2 expression is markedly reduced in the lung tissue of the chronic obstructive pulmonary disease (COPD) patients compared with the control group, which results in amplification of the inflammatory response with depressed activity of HDAC2 in peripheral lung and in alveolar macrophages of the patients correlated with severity of COPD (Barnes, 2009; Ito et al., 2005). Besides, reduced activity of HDAC2 is observed in alveolar macrophages isolated from patients with asthma or COPD, and the restoration of HDAC activity normalizes the cytokine responses of these macrophages in response to LPS (Cosio et al., 2004a, 2004b; Ito et al., 2006). Thus, our data provide a potential role of HDAC2 in regulation of chronic inflammation through regulation of major inflammatory cytokine IL-1 β by targeting NLRP3 inflammasome.

In this study we showed that *Mtb* infection increases the HDAC enzymatic activity. Previous studies demonstrated that compared with healthy subjects, PBMC from patients with active pulmonary TB disease have

decreased levels of acetylated H3K14, and this was reversed to normal after anti-TB treatment (Chen et al., 2017). In addition, it was demonstrated that TB patients with a low H3K14 acetylation had lower one-year survival than those with a high value (Chen et al., 2017). However, the inhibition of protein synthesis by cycloheximide markedly reduced the elevated levels of IL-1 β and NLRP3 mRNA induced by DHOB (Figures S5A and S5B), indicating that inhibition of HDAC2 activity may lead to increased NLRP3 expression and activation indirectly through new protein synthesis, which may be due to reduced repressor complex that requires HDAC2 for their activity, and reduced HDAC2 activity may compromise the repressor complex (Kim et al., 2020; Liu et al., 2020)-mediated suppression of major regulator of NLRP3 expression in innate immune cells.

Taken together, *Mtb* may induce H3K9/K14 deacetylation to silence host immune defense genes, such as IL-1 β for its immune evasion with the involvement of HDAC2 and that may also affect the development and clinical manifestation of TB infection because of its reduced expression that is supported by reduced expression of HDAC2 at mRNA level in PBMC of tuberculosis patients in comparison to LTBI subjects (Figure S6).

Clinical *Mtb* isolates induce differential IL-1 β secretion from cells, and it was demonstrated previously that it is not attributed to differential IL-1 β mRNA transcription or pro-IL-1 β accumulation but by modulation of pro-IL-1 β maturation pathways dependent on caspase-1 (Krishnan et al., 2013). Interestingly, another study demonstrated that the patients infected with low IL-1 β -inducing *Mtb* isolate had extensive lung pathology (Sousa et al., 2020). Thus, it is tempting to speculate that the HDAC2-mediated regulation of IL-1 β maturation through NLRP3 inflammasome activation may play a significant role in host immune defense against TB infection and disease manifestation, which warrant future studies.

In conclusion, we demonstrated that an epigenetic mechanism in host innate immune cells may play critical roles in regulation of IL-1 β production through HDAC2-mediated regulation of NLRP3 expression and inflammasome activation, and DHOB, a known HDAC1 inhibitor, targets HDAC2 as well.

Limitations of study

This study demonstrated that the epigenetic effector molecule HDAC2 regulates IL-1 β production by innate immune cells through the regulation of NLRP3 inflammasome activation in both *in vitro* and *in vivo* models. However, there are limitations in this study. Most of the studies were performed with primary immune cells in a healthy condition. To further establish the role of HDAC2 in regulation of IL-1 β production with disease relevance in our future studies, the significance of HDAC2-mediated regulation of IL-1 β production can be examined in murine models of TB infection with the cell-specific conditional deletion of HDAC2 to complement our observation with DHOB in a mouse model of TB infection. It is also desirable to study the expression and activity of HDACs with a focus on HDAC2 in TB patients and the patients with other chronic inflammatory diseases in correlation with IL-1 β production, disease severity, and response to therapy. These studies would further complement and establish the cell-specific role of HDAC2 in regulation of IL-1 β production by innate immune cells in the pathogenesis of specific diseases with chronic inflammation.

STAR★METHODS

Detailed methods are provided in the online version of this paper and include the following:

- KEY RESOURCES TABLE
- RESOURCE AVAILABILITY
 - Lead contact
 - Materials availability
 - Data and code availability
- EXPERIMENTAL MODELS AND SUBJECT DETAILS
 - Human subjects
 - Animals
 - Generation of human peripheral blood monocyte derived macrophages and dendritic cells
 - Generation of mouse bone marrow-derived macrophages and dendritic cells and culture
 - CRISPR/Cas9 mediated gene knockdown
 - Generation and culture of THP-1 macrophages

● **METHOD DETAILS**

- Chemical compounds
- *Mtb* infection and cell stimulation
- Aerosol infection of mice with *Mtb* and HDAC1 inhibitor treatment
- Cytokine assay
- Quantification of mRNA expression by real-time PCR
- Western blotting
- Cell viability
- Determination of ASC oligomerization by Western blotting
- HDAC activity assay
- Molecular docking studies
- Drug affinity responsive target stability assay

● **QUANTIFICATION AND STATISTICAL ANALYSIS**

SUPPLEMENTAL INFORMATION

Supplemental information can be found online at <https://doi.org/10.1016/j.isci.2022.104799>.

ACKNOWLEDGMENTS

We thank Dr. Amy Tvinnereim for her technical assistance in aerosol infection of the mice with H37Rv. This research is supported by the funds from the University of Texas Health Science Center at Tyler and the Cain Foundation for Infectious Disease Research.

AUTHOR CONTRIBUTIONS

JDM and BS designed and performed the experiments and analyzed and organized the experimental data. RV and BJ contributed to the interpretation of the results; JDM and BS wrote the manuscript and designed the figures. AI performed the docking studies. BS conceived and supervised the project, and all authors approved the final version of the manuscript.

DECLARATION OF INTERESTS

The authors have no financial conflicts of interest.

Received: March 30, 2022

Revised: June 11, 2022

Accepted: July 14, 2022

Published: August 19, 2022

REFERENCES

- Angioliilli, C., Kabala, P.A., Grabiec, A.M., Van Baarsen, I.M., Ferguson, B.S., García, S., Malvar Fernandez, B., McKinsey, T.A., Tak, P.P., Fossati, G., et al. (2017). Histone deacetylase 3 regulates the inflammatory gene expression programme of rheumatoid arthritis fibroblast-like synoviocytes. *Ann. Rheum. Dis.* 76, 277–285. <https://doi.org/10.1136/annrheumdis-2015-209064>.
- Arbibe, L., Kim, D.W., Batsche, E., Pedron, T., Mateescu, B., Muchardt, C., Parsot, C., and Sansonetti, P.J. (2007). An injected bacterial effector targets chromatin access for transcription factor NF-kappaB to alter transcription of host genes involved in immune responses. *Nat. Immunol.* 8, 47–56. <https://doi.org/10.1038/ni1423>.
- Aufhauser, D.D., Jr., Hernandez, P., Concors, S.J., O'Brien, C., Wang, Z., Murken, D.R., Samanta, A., Beier, U.H., Krumeich, L., Bhatti, T.R., et al. (2021). HDAC2 targeting stabilizes the CoREST complex in renal tubular cells and protects against renal ischemia/reperfusion injury. *Sci. Rep.* 11, 9018. <https://doi.org/10.1038/s41598-021-88242-3>.
- Barnes, P.J. (2009). Role of HDAC2 in the pathophysiology of COPD. *Annu. Rev. Physiol.* 71, 451–464. <https://doi.org/10.1146/annurev.physiol.010908.163257>.
- Bauer, S., Ratz, L., Heckmann-Nötzel, D., Kaczorowski, A., Hohenfellner, M., Kristiansen, G., Duensing, S., Altevogt, P., Klauk, S.M., and Sültmann, H. (2021). miR-449a repression leads to enhanced NOTCH signaling in TMPRSS2:ERG fusion positive prostate cancer cells. *Cancers* 13, 964. <https://doi.org/10.3390/cancers13050964>.
- Bauernfeind, F.G., Horvath, G., Stutz, A., Alnemri, E.S., MacDonald, K., Speert, D., Fernandes-Alnemri, T., Wu, J., Monks, B.G., Fitzgerald, K.A., et al. (2009). Cutting edge: NF-kappaB activating pattern recognition and cytokine receptors license NLRP3 inflammasome activation by regulating NLRP3 expression. *J. Immunol.* 183, 787–791. <https://doi.org/10.4049/jimmunol.0901363>.
- Bazou, D., Ng, M.R., Song, J.W., Chin, S.M., Maimon, N., and Munn, L.L. (2016). Flow-induced HDAC1 phosphorylation and nuclear export in angiogenic sprouting. *Sci. Rep.* 6, 34046. <https://doi.org/10.1038/srep34046>.
- Bellamy, R., Ruwende, C., Corrah, T., McAdam, K.P., Whittle, H.C., and Hill, A.V. (1998). Assessment of the interleukin 1 gene cluster and other candidate gene polymorphisms in host susceptibility to tuberculosis. *Tuber. Lung Dis.* 79, 83–89. <https://doi.org/10.1054/tuld.1998.0009>.
- Bierne, H., Hamon, M., and Cossart, P. (2012). Epigenetics and bacterial infections. *Cold Spring Harb. Perspect. Med.* 2, a010272. <https://doi.org/10.1101/cshperspect.a010272>.
- Cai, Y., Yang, Q., Tang, Y., Zhang, M., Liu, H., Zhang, G., Deng, Q., Huang, J., Gao, Z., Zhou, B., et al. (2014). Increased complement C1q level marks active disease in human tuberculosis. *PLoS One* 9, e92340. <https://doi.org/10.1371/journal.pone.0092340>.
- Chen, Y.C., Chao, T.Y., Leung, S.Y., Chen, C.J., Wu, C.C., Fang, W.F., Wang, Y.H., Chang, H.C.,

Wang, T.Y., Lin, Y.Y., et al. (2017). Histone H3K14 hypoacetylation and H3K27 hypermethylation along with HDAC1 up-regulation and KDM6B down-regulation are associated with active pulmonary tuberculosis disease. *Am. J. Transl. Res.* 9, 1943–1955.

Cosio, B.G., Mann, B., Ito, K., Jazrawi, E., Barnes, P.J., Chung, K.F., and Adcock, I.M. (2004a). Histone acetylase and deacetylase activity in alveolar macrophages and blood monocytes in asthma. *Am. J. Respir. Crit. Care Med.* 170, 141–147. <https://doi.org/10.1164/rccm.200305-659OC>.

Cosio, B.G., Tsaprouni, L., Ito, K., Jazrawi, E., Adcock, I.M., and Barnes, P.J. (2004b). Theophylline restores histone deacetylase activity and steroid responses in COPD macrophages. *J. Exp. Med.* 200, 689–695. <https://doi.org/10.1084/jem.20040416>.

Cox, D.J., Coleman, A.M., Gogan, K.M., Phelan, J.J., Ó Maoldomhnaigh, C., Dunne, P.J., Basdeo, S.A., and Keane, J. (2020). Inhibiting histone deacetylases in human macrophages promotes glycolysis, IL-1beta, and T helper cell responses to *Mycobacterium tuberculosis*. *Front. Immunol.* 11, 1609. <https://doi.org/10.3389/fimmu.2020.01609>.

Ding, S.Z., Fischer, W., Kaparakis-Liaskos, M., Liechti, G., Merrell, D.S., Grant, P.A., Ferrero, R.L., Crowe, S.E., Haas, R., Hatakeyama, M., and Goldberg, J.B. (2010). Helicobacter pylori-induced histone modification, associated gene expression in gastric epithelial cells, and its implication in pathogenesis. *PLoS One* 5, e9875. <https://doi.org/10.1371/journal.pone.0009875>.

Dorhoi, A., Nouailles, G., Jörg, S., Hagens, K., Heinemann, E., Pradi, L., Oberbeck-Müller, D., Duque-Correa, M.A., Reece, S.T., Ruland, J., et al. (2012). Activation of the NLRP3 inflammasome by *Mycobacterium tuberculosis* is uncoupled from susceptibility to active tuberculosis. *Eur. J. Immunol.* 42, 374–384. <https://doi.org/10.1002/eji.201141548>.

Feng, Y., Kong, Y., Barnes, P.F., Huang, F.F., Klucar, P., Wang, X., Samten, B., Sengupta, M., Machona, B., Donis, R., et al. (2011). Exposure to cigarette smoke inhibits the pulmonary T-cell response to influenza virus and *Mycobacterium tuberculosis*. *Infect. Immun.* 79, 229–237. <https://doi.org/10.1128/IAI.00709-10>.

Fremont, C.M., Togbe, D., Doz, E., Rose, S., Vasseur, V., Maillet, I., Jacobs, M., Ryffel, B., and Quesniaux, V.F.J. (2007). IL-1 receptor-mediated signal is an essential component of MyD88-dependent innate response to *Mycobacterium tuberculosis* infection. *J. Immunol.* 179, 1178–1189. <https://doi.org/10.4049/jimmunol.179.2.1178>.

García-García, J.C., Barat, N.C., Trembley, S.J., and Dumler, J.S. (2009). Epigenetic silencing of host cell defense genes enhances intracellular survival of the rickettsial pathogen *Anaplasma phagocytophilum*. *PLoS Pathog.* 5, e1000488. <https://doi.org/10.1371/journal.ppat.1000488>.

Gregoret, I.V., Lee, Y.M., and Goodson, H.V. (2004). Molecular evolution of the histone deacetylase family: functional implications of phylogenetic analysis. *J. Mol. Biol.* 338, 17–31. <https://doi.org/10.1016/j.jmb.2004.02.006>.

Grozinger, C.M., and Schreiber, S.L. (2002). Deacetylase enzymes. *Chem. Biol.* 9, 3–16. [https://doi.org/10.1016/s1074-5521\(02\)00092-3](https://doi.org/10.1016/s1074-5521(02)00092-3).

Hamon, M.A., and Cossart, P. (2011). K+ efflux is required for histone H3 dephosphorylation by *Listeria monocytogenes* listeriolysin O and other pore-forming toxins. *Infect. Immun.* 79, 2839–2846. <https://doi.org/10.1128/IAI.01243-10>.

Ito, K., Ito, M., Elliott, W.M., Cosio, B., Caramori, G., Kon, O.M., Barczyk, A., Hayashi, S., Adcock, I.M., Hogg, J.C., and Barnes, P.J. (2005). Decreased histone deacetylase activity in chronic obstructive pulmonary disease. *N. Engl. J. Med.* 352, 1967–1976. <https://doi.org/10.1056/NEJMoa041892>.

Ito, K., Yamamura, S., Essilfie-Quaye, S., Cosio, B., Ito, M., Barnes, P.J., and Adcock, I.M. (2006). Histone deacetylase 2-mediated deacetylation of the glucocorticoid receptor enables NF-kappaB suppression. *J. Exp. Med.* 203, 7–13. <https://doi.org/10.1084/jem.20050466>.

Jose, L., Ramachandran, R., Bhagavat, R., Gomez, R.L., Chandran, A., Raghunandan, S., Omkumar, R.V., Chandra, N., Mundayoor, S., and Kumar, R.A. (2016). Hypothetical protein Rv3423.1 of *Mycobacterium tuberculosis* is a histone acetyltransferase. *FEBS J.* 283, 265–281. <https://doi.org/10.1111/febs.13566>.

Juffermans, N.P., Florquin, S., Camoglio, L., Verbon, A., Kolk, A.H., Speelman, P., van Deventer, S.J., and van Der Poll, T. (2000). Interleukin-1 signaling is essential for host defense during murine pulmonary tuberculosis. *J. Infect. Dis.* 182, 902–908. <https://doi.org/10.1086/315771>.

Jung, B.G., Vankayalapati, R., and Samten, B. (2021). *Mycobacterium tuberculosis* stimulates IL-1beta production by macrophages in an ESAT-6 dependent manner with the involvement of serum amyloid A3. *Mol. Immunol.* 135, 285–293. <https://doi.org/10.1016/j.molimm.2021.04.022>.

Jung, B.G., Wang, X., Yi, N., Ma, J., Turner, J., and Samten, B. (2017). Early secreted antigenic target of 6-kDa of *Mycobacterium tuberculosis* stimulates IL-6 production by macrophages through activation of STAT3. *Sci. Rep.* 7, 40984. <https://doi.org/10.1038/srep40984>.

Kim, M.Y., Yan, B., Huang, S., and Qiu, Y. (2020). Regulating the regulators: the role of histone deacetylase 1 (HDAC1) in erythropoiesis. *Int. J. Mol. Sci.* 21, 8460. <https://doi.org/10.3390/ijms21228460>.

Krishnan, N., Robertson, B.D., and Thwaites, G. (2013). Pathways of IL-1beta secretion by macrophages infected with clinical *Mycobacterium tuberculosis* strains. *Tuberculosis* 93, 538–547. <https://doi.org/10.1016/j.tube.2013.05.002>.

Lai, Y., Babunovic, G.H., Cui, L., Dedon, P.C., Doench, J.G., Fortune, S.M., and Lu, T.K. (2020). Illuminating host-mycobacterial interactions with genome-wide CRISPR knockout and CRISPRi screens. *Cell Syst.* 11, 239–251.e7. e237. <https://doi.org/10.1016/j.cels.2020.08.010>.

Lecoeur, H., Prina, E., Rosazza, T., Kokou, K., N'Diaye, P., Aulner, N., Varet, H., Bussotti, G., Xing, Y., Milon, G., et al. (2020). Targeting macrophage histone H3 modification as a

Leishmania strategy to dampen the NF-kappaB/NLRP3-Mediated inflammatory response. *Cell Rep.* 30, 1870–1882.e4. <https://doi.org/10.1016/j.celrep.2020.01.030>.

Li, S., Fossati, G., Marchetti, C., Modena, D., Pozzi, P., Reznikov, L.L., Moras, M.L., Azam, T., Abbate, A., Mascagni, P., and Dinarello, C.A. (2015). Specific inhibition of histone deacetylase 8 reduces gene expression and production of proinflammatory cytokines in vitro and in vivo. *J. Biol. Chem.* 290, 2368–2378. <https://doi.org/10.1074/jbc.M114.618454>.

Liu, C.C., Huang, Z.X., Li, X., Shen, K.F., Liu, M., Ouyang, H.D., Zhang, S.B., Ruan, Y.T., Zhang, X.L., Wu, S.L., et al. (2018). Upregulation of NLRP3 via STAT3-dependent histone acetylation contributes to painful neuropathy induced by bortezomib. *Exp. Neurol.* 302, 104–111. <https://doi.org/10.1016/j.expneurol.2018.01.011>.

Liu, T., Wan, Y., Xiao, Y., Xia, C., and Duan, G. (2020). Dual-target inhibitors based on HDACs: novel antitumor agents for cancer therapy. *J. Med. Chem.* 63, 8977–9002. <https://doi.org/10.1021/acs.jmedchem.0c00491>.

Lomenick, B., Hao, R., Jonai, N., Chin, R.M., Aghajan, M., Warburton, S., Wang, J., Wu, R.P., Gomez, F., Loo, J.A., et al. (2009). Target identification using drug affinity responsive target stability (DARTS). *Proc. Natl. Acad. Sci. USA* 106, 21984–21989. <https://doi.org/10.1073/pnas.0910040106>.

Lugrin, J., and Martinon, F. (2017). Detection of ASC oligomerization by western blotting. *Bio. Protoc.* 7, e2292. <https://doi.org/10.21769/BioProtoc.2292>.

Martinon, F., and Tschopp, J. (2007). Inflammatory caspases and inflammasomes: master switches of inflammation. *Cell. Death. Differ.* 14, 10–22. <https://doi.org/10.1038/sj.cdd.4402038>.

Mayer-Barber, K.D., Andrade, B.B., Barber, D.L., Hieny, S., Feng, C.G., Caspar, P., Oland, S., Gordon, S., and Sher, A. (2011). Innate and adaptive interferons suppress IL-1alpha and IL-1beta production by distinct pulmonary myeloid subsets during *Mycobacterium tuberculosis* infection. *Immunity* 35, 1023–1034. <https://doi.org/10.1016/j.immuni.2011.12.002>.

Mayer-Barber, K.D., Barber, D.L., Shenderov, K., White, S.D., Wilson, M.S., Cheever, A., Kugler, D., Hieny, S., Caspar, P., Núñez, G., et al. (2010). Caspase-1 independent IL-1beta production is critical for host resistance to mycobacterium tuberculosis and does not require TLR signaling in vivo. *J. Immunol.* 184, 3326–3330. <https://doi.org/10.4049/jimmunol.0904189>.

McElvania Tekippe, E., Allen, I.C., Hulseberg, P.D., Sullivan, J.T., McCann, J.R., Sandor, M., Braunstein, M., and Ting, J.P.Y. (2010). Granuloma formation and host defense in chronic *Mycobacterium tuberculosis* infection requires PYCARD/ASC but not NLRP3 or caspase-1. *PLoS One* 5, e12320. <https://doi.org/10.1371/journal.pone.0012320>.

Mishra, B.B., Moura-Alves, P., Sonawane, A., Hacoheh, N., Griffiths, G., Moita, L.F., and Anes, E. (2010). *Mycobacterium tuberculosis* protein ESAT-6 is a potent activator of the NLRP3/ASC inflammasome. *Cell. Microbiol.* 12,

1046–1063. <https://doi.org/10.1111/j.1462-5822.2010.01450.x>.

Mishra, B.B., Rathinam, V.A.K., Martens, G.W., Martinot, A.J., Kornfeld, H., Fitzgerald, K.A., and Sasseti, C.M. (2013). Nitric oxide controls the immunopathology of tuberculosis by inhibiting NLRP3 inflammasome-dependent processing of IL-1 β . *Nat. Immunol.* *14*, 52–60. <https://doi.org/10.1038/ni.2474>.

Moon, B.-S., Yun, H.-M., Chang, W.-H., Steele, B.H., Cai, M., Choi, S.H., and Lu, W. (2017). Smek promotes corticogenesis through regulating Mbd3's stability and Mbd3/NuRD complex recruitment to genes associated with neurogenesis. *PLoS Biol.* *15*, e2001220. <https://doi.org/10.1371/journal.pbio.2001220>.

Moreira, J.D., Koch, B.E.V., van Veen, S., Walburg, K.V., Vrieling, F., Mara Pinto Dabés Guimarães, T., Meijer, A.H., Spaik, H.P., Ottenhoff, T.H.M., Haks, M.C., and Heemskerk, M.T. (2020). Functional inhibition of host histone deacetylases (HDACs) enhances in vitro and in vivo antimycobacterial activity in human macrophages and in zebrafish. *Front. Immunol.* *11*, 36. <https://doi.org/10.3389/fimmu.2020.00036>.

Moreno-Yruela, C., Zhang, D., Wei, W., Bæk, M., Liu, W., Gao, J., Danková, D., Nielsen, A.L., Bolding, J.E., Yang, L., et al. (2022). Class I histone deacetylases (HDAC1-3) are histone lysine deacetylases. *Sci. Adv.* *8*, eabi6696. <https://doi.org/10.1126/sciadv.abi6696>.

Nusinzon, I., and Horvath, C.M. (2003). Interferon-stimulated transcription and innate antiviral immunity require deacetylase activity and histone deacetylase 1. *Proc. Natl. Acad. Sci. USA* *100*, 14742–14747. <https://doi.org/10.1073/pnas.2433987100>.

Pai, M.Y., Lomenick, B., Hwang, H., Schiestl, R., McBride, W., Loo, J.A., and Huang, J. (2015). Drug affinity responsive target stability (DARTS) for small-molecule target identification. In *Chemical Biology* (Springer), pp. 287–298. https://doi.org/10.1007/978-1-4939-2269-7_22.

Park, S.Y., and Kim, J.S. (2020). A short guide to histone deacetylases including recent progress on class II enzymes. *Exp. Mol. Med.* *52*, 204–212. <https://doi.org/10.1038/s12276-020-0382-4>.

Patel, U., Rajasingh, S., Samanta, S., Cao, T., Dawn, B., and Rajasingh, J. (2017). Macrophage polarization in response to epigenetic modifiers during infection and inflammation. *Drug. Discov. Today.* *22*, 186–193. <https://doi.org/10.1016/j.drudis.2016.08.006>.

Roger, T., Lugin, J., Le Roy, D., Goy, G., Mombelli, M., Koessler, T., Ding, X.C., Chanson, A.L., Reymond, M.K., Miconnet, I., et al. (2011). Histone deacetylase inhibitors impair innate immune responses to Toll-like receptor agonists and to infection. *Blood* *117*, 1205–1217. <https://doi.org/10.1182/blood-2010-05-284711>.

Sahu, M., and Sahu, A. (2015). Leptin receptor expressing neurons express phosphodiesterase-3B (PDE3B) and leptin induces STAT3 activation

in PDE3B neurons in the mouse hypothalamus. *Peptides* *73*, 35–42. <https://doi.org/10.1016/j.peptides.2015.08.011>.

Savelyeva, I., and Dobbstein, M. (2011). Infection with E1B-mutant adenovirus stabilizes p53 but blocks p53 acetylation and activity through E1A. *Oncogene* *30*, 865–875. <https://doi.org/10.1038/onc.2010.461>.

Seshadri, C., Sedaghat, N., Campo, M., Peterson, G., Wells, R.D., Olson, G.S., Sherman, D.R., Stein, C.M., Mayanja-Kizza, H., Shojaie, A., et al. (2017). Transcriptional networks are associated with resistance to Mycobacterium tuberculosis infection. *PLoS One* *12*, e0175844. <https://doi.org/10.1371/journal.pone.0175844>.

Sousa, J., Ca, B., Maceiras, A.R., Simões-Costa, L., Fonseca, K.L., Fernandes, A.I., Ramos, A., Carvalho, T., Barros, L., Magalhães, C., et al. (2020). Mycobacterium tuberculosis associated with severe tuberculosis evades cytosolic surveillance systems and modulates IL-1 β production. *Nat. Commun.* *11*, 1949. <https://doi.org/10.1038/s41467-020-15832-6>.

Stammler, D., Eigenbrod, T., Menz, S., Frick, J.S., Sweet, M.J., Shakespear, M.R., Jantsch, J., Siegert, I., Wölfl, S., Langer, J.D., et al. (2015). Inhibition of histone deacetylases permits lipopolysaccharide-mediated secretion of bioactive IL-1 β via a caspase-1-independent mechanism. *J. Immunol.* *195*, 5421–5431. <https://doi.org/10.4049/jimmunol.1501195>.

Swanson, K.V., Deng, M., and Ting, J.P.Y. (2019). The NLRP3 inflammasome: molecular activation and regulation to therapeutics. *Nat. Rev. Immunol.* *19*, 477–489. <https://doi.org/10.1038/s41577-019-0165-0>.

Thiagalingam, S., Cheng, K.H., Lee, H.J., Mineva, N., Thiagalingam, A., and Ponte, J.F. (2003). Histone deacetylases: unique players in shaping the epigenetic histone code. *Ann. N.Y. Acad. Sci.* *983*, 84–100. <https://doi.org/10.1111/j.1749-6632.2003.tb05964.x>.

Trott, O., and Olson, A.J. (2010). AutoDock Vina: improving the speed and accuracy of docking with a new scoring function, efficient optimization, and multithreading. *J. Comput. Chem.* *31*, 455–461. <https://doi.org/10.1002/jcc.21334>.

Tsao, T.C., Hong, J., Huang, C., Yang, P., Liao, S.K., and Chang, K.S. (1999). Increased TNF- α , IL-1 β and IL-6 levels in the bronchoalveolar lavage fluid with the upregulation of their mRNA in macrophages lavaged from patients with active pulmonary tuberculosis. *Tuber. Lung Dis.* *79*, 279–285. <https://doi.org/10.1054/tuld.1999.0215>.

Wagner, F.F., Zhang, Y.L., Fass, D.M., Joseph, N., Gale, J.P., Weiwer, M., McCarren, P., Fisher, S.L., Kaya, T., Zhao, W.N., et al. (2015). Kinetically selective inhibitors of histone deacetylase 2 (HDAC2) as cognition enhancers. *Chem. Sci.* *6*, 804–815. <https://doi.org/10.1039/C4SC02130D>.

Walter, K., Hölscher, C., Tschopp, J., and Ehlers, S. (2010). NALP3 is not necessary for early protection against experimental tuberculosis. *Immunobiology* *215*, 804–811. <https://doi.org/10.1016/j.jmbio.2010.05.015>.

Wang, X., Barnes, P.F., Dobos-Elder, K.M., Townsend, J.C., Chung, Y.T., Shams, H., Weis, S.E., and Samten, B. (2009). ESAT-6 inhibits production of IFN- γ by Mycobacterium tuberculosis-responsive human T cells. *J. Immunol.* *182*, 3668–3677. <https://doi.org/10.4049/jimmunol.0803579>.

Wang, X., Barnes, P.F., Huang, F., Alvarez, I.B., Neuenschwander, P.F., Sherman, D.R., and Samten, B. (2012). Early secreted antigenic target of 6-kDa protein of Mycobacterium tuberculosis primes dendritic cells to stimulate Th17 and inhibit Th1 immune responses. *J. Immunol.* *189*, 3092–3103. <https://doi.org/10.4049/jimmunol.1200573>.

Wang, Y., Curry, H.M., Zwilling, B.S., and Lafuse, W.P. (2005). Mycobacteria inhibition of IFN- γ induced HLA-DR gene expression by up-regulating histone deacetylation at the promoter region in human THP-1 monocytic cells. *J. Immunol.* *174*, 5687–5694. <https://doi.org/10.4049/jimmunol.174.9.5687>.

Wei, M., Wang, L., Wu, T., Xi, J., Han, Y., Yang, X., Zhang, D., Fang, Q., and Tang, B. (2016). NLRP3 activation was regulated by DNA methylation modification during Mycobacterium tuberculosis infection. *BioMed Res. Int.* *4323281*. <https://doi.org/10.1155/2016/4323281>.

WHO (2018). Antimicrobial Resistance: World Health Organization. <https://www.who.int/en/news-room/fact-sheets/detail/antimicrobial-resistance>.

Wilkinson, R.J., Patel, P., Llewelyn, M., Hirsch, C.S., Pasvol, G., Snounou, G., Davidson, R.N., and Toossi, Z. (1999). Influence of polymorphism in the genes for the interleukin (IL)-1 receptor antagonist and IL-1 β on tuberculosis. *J. Exp. Med.* *189*, 1863–1874. <https://doi.org/10.1084/jem.189.12.1863>.

Winchell, C.G., Mishra, B.B., Phuah, J.Y., Saqib, M., Nelson, S.J., Maiello, P., Causgrove, C.M., Ameal, C.L., Stein, B., Borish, H.J., et al. (2020). Evaluation of IL-1 blockade as an adjunct to linezolid therapy for tuberculosis in mice and macaques. *Front. Immunol.* *11*, 891. <https://doi.org/10.3389/fimmu.2020.00891>.

Wu, S., Ye, Z., Liu, X., Zhao, Y., Xia, Y., Steiner, A., Petrof, E.O., Claud, E.C., and Sun, J. (2010). Salmonella typhimurium infection increases p53 acetylation in intestinal epithelial cells. *Am. J. Physiol. Gastrointest. Liver. Physiol.* *298*, G784–G794. <https://doi.org/10.1152/ajpgi.00526.2009>.

Zhang, G., Zhou, B., Li, S., Yue, J., Yang, H., Wen, Y., Zhan, S., Wang, W., Liao, M., Zhang, M., et al. (2014). Allele-specific induction of IL-1 β expression by C/EBP β and PU.1 contributes to increased tuberculosis susceptibility. *PLoS Pathog.* *10*, e1004426. <https://doi.org/10.1371/journal.ppat.1004426>.

STAR★METHODS

KEY RESOURCES TABLE

REAGENT OR RESOURCE	SOURCE	IDENTIFIER
<i>Antibodies</i>		
Anti-HDAC1 (D5C6U)	Cell Signaling	Cat: #34589, RRID:AB_2756821
Anti-HDAC2 (D6S5P)	Cell Signaling	Cat# 57,156, RRID:AB_2756828)
Anti-HDAC3 (D2O1K)	Cell Signaling	Cat# 85,057, RRID:AB_2800047
Anti-NLRP3 (D4D8T)	Cell Signaling	Cat# 15,101, RRID:AB_2722591
Anti-IL-1 β (D3U3E)	Cell Signaling	Cat# 12,703, RRID:AB_2737350
Anti-Histone H3	Cell Signaling	Cat# 9715, RRID:AB_331563
Anti-Acetyl-Histone H3 (Lys9/Lys14)	Cell Signaling	Cat# 9677, RRID:AB_1147653
Anti-Caspase-1 (D7F10)	Cell Signaling	Cat# 3866, RRID:AB_2069051
Anti-ASC/TMS1 (E1E3I)	Cell Signaling	Cat# 13,833, RRID:AB_2798325
Anti-GAPDH Antibody (0411)	Santa Cruz Biotechnology	Cat# sc-47724, RRID:AB_627678
Anti- β -Actin	Santa Cruz Biotechnology	Cat# sc-47778 HRP, RRID:AB_2714189
<i>Critical commercial assays</i>		
Epigenase HDAC Activity/Inhibition Direct Assay Kit	Epigentek	Cat: P-4034
Human IL-1 β ELISA BASIC kit (HRP)	Mabtech	Cat: 3416-1H-20
ELISA MAX [™] Standard Set Human IL-6	Biolegend	Cat: 430,501
TNF alpha (Total) Human ELISA Kit	Invitrogen	Cat: 50-179-28
<i>Chemicals, peptides, and recombinant proteins</i>		
4-(dimethylamino)-N-[6-(hydroxyamino)-6-oxohexyl]-benzamide CAS number (193,551-00-7)	Santa Cruz Biotechnology	Cat: sc-223859
MS-275 CAS number (209,783-80-2)	Cayman Chemical	Cat: 18,287
Mocetinostat CAS Number (726,169-73-9)	Cayman Chemical	Cat: 13,284
RGFP966 CAS Number (1,357,389-11-7)	Cayman Chemical	Cat: 16,917
TMP-195 CAS Number (1,314,891-22-9)	Cayman Chemical	Cat: 23,242
BRD73954 CAS Number (1,440,209-96-0)	Cayman Chemical	Cat: 16,919
Trichostatin A CAS Number (58,880-19-6)	Cayman Chemical	Cat: 89,730
BRD6688 CAS Number (1,404,562-17-9)	Cayman Chemical	Cat: 19,836
Caspase-1 Inhibitor II CAS number (178,603-78-6)	Sigma Aldrich	Cat: 400,012
NLRP3 Inhibitor, MCC950 CAS Number (256,373-96-3)	Sigma Aldrich	Cat: 5.38120
Cycloheximide CAS Number (66-81-9)	Sigma Aldrich	Cat: 239,763
MTT- Thiazolyl Blue Tetrazolium Bromide	Affymetrix	Cat: 19265
DSP [dithiobis(succinimidyl propionate)]	Thermo Fisher	Cat: 22586
Recombinant Murine IFN- γ	PeproTech, Inc	Cat: AF-315-05
Lipopolysaccharide, Ultra Pure, Salmonella minnesota R595	Sigma Aldrich	Cat: 437628
Pronase	Sigma Aldrich	Cat: 10165921001
Deacetylation Inhibition Cocktail	Santa Cruz Biotechnology	Cat: sc-362323
Protease Inhibitor Cocktail	Sigma Aldrich	Cat: P1860

(Continued on next page)

Continued

REAGENT OR RESOURCE	SOURCE	IDENTIFIER
CD40LT	Immunex Corporation	N/A
Lipofectamine™ CRISPRMAX™ Cas9 Transfection Reagent	Invitrogen	Cat: CMAX00001
Oligonucleotides		
TrueGuide Synthetic gRNA HDAC1 (CRISPR1087187_SGM)	Invitrogen	Cat: A35533
TrueGuide Synthetic gRNA HDAC2 (CRISPR1097138_SGM)	Invitrogen	Cat: A35533
TrueGuide Synthetic gRNA HDAC2 (CRISPR1097140_SGM)	Invitrogen	Cat: A35533
non-targeting control synthetic gRNA (CRISPR1097141_SGM)	Invitrogen	Cat: A35533
Hs00918082_m1 (NLRP3)	Invitrogen	Cat: 4331182
Mm00840904_m1 (NLRP3)	Invitrogen	Cat: 4331182
Hs01555410_m1 (IL1B)	Invitrogen	Cat: 4331182
Hs99999901_s1 (18S)	Invitrogen	Cat: 4331182
Mm99999915_g1 (Gapdh)	Invitrogen	Cat: 4331182
Experimental models: Organisms/strain		
Mouse: C57BL/6 (Female)	Jackson Lab	Cat: 664
<i>Mycobacterium tuberculosis</i> (H37Rv)	Dr. David Sherman (University of Washington, Seattle, WA)	N/A
<i>Mycobacterium tuberculosis</i> (H37Rv::Δ3875)	Dr. David Sherman (University of Washington, Seattle, WA)	N/A
<i>Mycobacterium tuberculosis</i> (H37Rv::Δ3875C)	Dr. David Sherman (University of Washington, Seattle, WA)	N/A

RESOURCE AVAILABILITY

Lead contact

For information and requests for the reagents, please contact and will be fulfilled by the corresponding author Buka Samten (buka.samten@uthct.edu).

Materials availability

This study did not generate new unique reagents.

Data and code availability

Data presented in this manuscript will be shared by the corresponding author upon request.

This paper does not report original code.

Any additional information required to reanalyze the data reported in this paper is available from the corresponding author upon contact.

EXPERIMENTAL MODELS AND SUBJECT DETAILS

Human subjects

QuantiFERON TB Gold negative or positive adult healthy donors were recruited for the collection of blood samples for this study following the protocols approved by the Institutional Review Board of the University of Texas Health Science Center at Tyler. All the participants were consented with signed documentation before the collection of blood samples.

Animals

Female 6-8 weeks old C57BL/6 mice were purchased from the Jackson Laboratory and housed at the animal facility of the University of Texas Health Science Center at Tyler. All the animal studies were performed in compliance with the NIH guidelines and regulations and approved by the Institutional Animal Care and Use Committee of the University of Texas Health Science Center at Tyler. All mice were maintained on a standard rodent chow diet (LabDiet, catalog 5053, 4.07 kcal/gm) for the entirety of the studies. After Mtb infection, all mice were housed and grouped randomly at 5 animals per cage in high-efficiency particulate air (HEPA) filtered racks in certified animal biosafety level 3 laboratories.

Generation of human peripheral blood monocyte derived macrophages and dendritic cells

Peripheral blood mononuclear cells (PBMC) were isolated by differential centrifugation of heparinized blood over Ficoll-Paque (GE Healthcare Life Science) and monocytes were sorted using anti-human CD14 mAb conjugated magnetic beads (Miltenyi Biotec, Bergisch Gladbach, Germany). The purity of the cells was > 98%, as determined by immunolabeling for CD14 and flow cytometry analysis for human peripheral blood monocytes with an Attune NxT Flow Cytometer (Thermo Fisher Scientific). The monocytes were cultured at 5×10^5 per well in 1 ml culture volume in a 24-well tissue culture plate or 2×10^6 cells/ml in a 12-well tissue culture plate in 2 ml RPMI-1640 medium (Thermo Fisher Scientific), supplemented with 5% heat-inactivated pooled human AB serum, 100 units/ml penicillin, 100 μ g/ml streptomycin, 1 mM sodium pyruvate, 0.1 mM MEM nonessential amino acids (all from Invitrogen) and cultured for 6 days to differentiate into monocyte derived macrophages (MDM). Human monocyte derived dendritic cells (MDDC) were generated by culturing with human granulocyte-macrophage-colony-stimulating factor (GM-CSF) and IL-4 (both from R&D systems) as described previously (Wang et al., 2009) by culturing for 5-6 days. Before infection or stimulation, the cells were rested overnight in the fresh culture medium without serum and cytokines.

Generation of mouse bone marrow-derived macrophages and dendritic cells and culture

Mouse bone marrow derived macrophages (BMDM) were generated from the bone marrow of the 6-8 weeks old female mice as described previously (Jung et al., 2017) by flushing out the bone marrow mouse femur and tibia. After red blood cell lyses, the cells were plated at 4×10^6 cells in a petri dish in 10 ml Dulbecco's Modified Eagle Medium/Nutrient Mixture (DMEM) F-12 (Thermo Fisher Scientific) containing 10% fetal bovine serum, 100 units/ml penicillin and 100 μ g/ml streptomycin and supplemented with 20% (v/v) L-929-conditional media. On day 3, another 5 ml of fresh DMEM/F12 medium with 20% conditional media were added and cultured for up to 7 days.

For the generation of bone marrow derived dendritic cells (BMDD), the bone marrow cells were cultured in tissue culture plates with supplemented with 10% FBS (Atlanta Biologicals, Atlanta, GA, US) containing 20 ng/ml of mouse recombinant GM-CSF and IL-4 (both from R&D systems) for 6-7 days. Three days after incubation, half of the cell culture medium was carefully removed and replenished with new DMEM/F12 medium containing 10% FBS and 20 ng/ml GM-CSF and IL-4. Before the stimulation or infection, the cells were rested overnight in the fresh culture medium without serum, cytokines, and conditional medium.

CRISPR/Cas9 mediated gene knockdown

THP-1 cells expressing Cas9 (Lai et al., 2020), generously provided by Dr. Timothy K. Lu from the Massachusetts Institute of Technology (Cambridge, MA), were plated in a 24-well plate at 5×10^4 cells/well in serum and antibiotic free RPMI-1640 medium with L-glutamine. For genomic editing, 7.5 pM of TrueGuide Synthetic gRNA (sgRNA) HDAC1 (CRISPR1087187_SGM), 7.5 pM of TrueGuide Synthetic gRNA (sgRNA) HDAC2 (CRISPR1097138_SGM and CRISPR1097140_SGM) or non-targeting control synthetic gRNA (csgRNA) were mixed with 1.5 μ l of Lipofectamine™ CRISPRMAX™ Cas9 Transfection Reagent (all from Invitrogen) in 50 μ l of Opti-MEM™ I Medium and incubated for 10 min at 37°C before adding into the cells. After overnight incubation, the cell culture medium was replaced with fresh RPMI-1640 with L-glutamine, supplemented with 10% heat-inactivated fetal bovine serum, 100 units/ml penicillin, 100 μ g/ml streptomycin, 1 mM sodium pyruvate, 0.1 mM MEM nonessential amino acids (all from Invitrogen). Three weeks after transfection, the efficiency of deletion at protein levels was determined by evaluation of the protein expression in cell protein extracts by western blotting using anti-HDAC1 or HDAC2 (Cell Signaling Technology).

Generation and culture of THP-1 macrophages

The control sgRNA transfected cells, the HDAC1 knockdown (KD) and HDAC2 KD THP-1 cells were differentiated into macrophages by two-day incubation in RPMI-1640 containing 20 ng/mL PMA. The macrophages were rested in FBS free RPMI-1640 for 24 hours before infection with H37Rv at 5 multiplicity of infection (MOI) for 3 hours at 37°C. The cells were then treated with DHOB for 1 hour and stimulated with 100 ng/ml ultrapure LPS (InvivoGene) plus 2.5 µg/ml CD40LT (Immunex) for 16 hours.

METHOD DETAILS

Chemical compounds

Pan-HDAC inhibitor Trichostatin A (TSA), class IIa HDAC inhibitors (HDAC4,5,7 and 9) TMP195, Class I & IV HDAC inhibitor (HDAC1,2,3 and 11) Mocetinostat, HDAC6 and 8 inhibitor BRD73954, HDAC3 inhibitor RGFP966 and a HDAC1 and 2 inhibitor BRD6688 were purchased from Cayman Chemical, HDAC1 and 3 inhibitor MS-275, and HDAC1 inhibitor 4-(dimethylamino)-N-[6-(hydroxyamino)-6-oxohexyl]-benzamide (DHOB) were purchased from Santa Cruz Biotechnology, NLRP3 specific inhibitor CP-456773/MCC 950, caspase-1 inhibitor caspase-1 Inhibitor II and protein synthesis inhibitor, cycloheximide, and pronase were purchased from Sigma-Aldrich. The stocks of all the chemical inhibitors were prepared in DMSO following the instructions of the vendors and stored at -80°C before use.

Mtb infection and cell stimulation

Mtb strain H37Rv, its *esat-6* deletion mutant (H37Rv:ΔRv3875) and the mutant strain complemented with *esat-6* gene (H37Rv:ΔRv3875C), provided by Dr. David Sherman (University of Washington, Seattle, WA), were cultured in 7H9 broth supplemented with 10% enrichment ADC (Remel) for 2-3 weeks to have the bacilli grown logarithmically, and prepared for infection as previously described (Wang et al., 2012). The bacteria were collected and washed with 10 ml HBSS once. After removal of the supernatant, the bacilli were resuspended in 5 ml HBSS and sonicated thrice with microtip sonicator. The sonicated bacilli were spun down at 1,100 rpm to pellet the remaining bacilli clumps and the upper part of the bacilli suspension was collected and quantified by determining the OD₆₀₀ with a photo spectrometry and determining the concentration of the bacilli using formula: number of bacilli/ml=OD₆₀₀ × 3 × 10⁸ × dilution factor. Macrophages or DCs were infected with freshly prepared *Mtb* strains at 5 or 10 MOI. At 3 h post infection the cells were treated with HDAC inhibitors for 1 hour and then stimulated with LPS and CD40LT as above or 25 ng/ml IFN-γ (PeproTech, Rock Hill, NJ) plus 100 ng/ml ultra-pure LPS. DMSO at the same dilutions with HDAC inhibitors was used as vehicle control. After 16-hour incubation, cell free culture supernatants were collected and stored at -80°C before the determination of the cytokine levels.

Aerosol infection of mice with Mtb and HDAC1 inhibitor treatment

Mice were infected with low dose H37Rv by an aerosolizer as described by us (Feng et al., 2011) to deposit about 25-50 CFU per lung. The next day, the homogenized whole lungs of 3 mice were plated on 7H10 agar plates and incubated at 37°C with 5% CO₂ for 3 weeks to determine the number of bacilli deposited in the lungs by aerosol infection. HDAC1 inhibitor DHOB was dissolved in DMSO at 16.7 µg/µl and stored at -80°C. The stocks were thawed and diluted in 0.9% sterile normal saline to have a desired dose (5 mg/kg body weight) in 100 µl of volume and administered by intraperitoneal (IP) injection. The same dilution of DMSO in 100 µl of saline (5.4%) was used as a vehicle control. The vehicle control or DHOB was administered daily for 6 days a week for two weeks. Then, the mice were sacrificed, and the lung tissues were passed through an 80 µm cell strainer to make single cell suspension in 2 ml HBSS. The lung homogenates were centrifuged at 5,000×g for 10 minutes at 4°C and the supernatants were collected into clean microcentrifuge tubes and stored at -80°C for cytokine analysis. The total RNA was extracted from a section of lung tissue using Trizol LS reagent (Invitrogen) for mRNA expression analysis.

Cytokine assay

The cytokine levels in the cell-free culture supernatants and the mice lung homogenates were determined by ELISA kits for human IL-1β (Mabtech) or mouse IL-1β (Biologend), IL-6 (BioLegend), and human TNF-α (BD Biotechnology) or mouse TNF-α (Biologend) according to the manufacturer's protocol.

Quantification of mRNA expression by real-time PCR

Total RNAs were extracted from DC at the end of culture and lung tissues with Trizol reagent. The RNAs were reverse transcribed to cDNA and the relative mRNA expression levels of human IL-1β, caspase-1

and NLRP3 were determined by Real-Time PCR as previously described (Wang et al., 2009) using primer and probe sets (ThermoFisher Scientific) and using human 18S rRNA or mouse GAPDH as internal controls for sample normalization. The mRNA levels were expressed as fold change over the cells without stimulation or infection.

Western blotting

The expression of the proteins in macrophages and DC were determined by western blotting from the whole cell protein extracts (protein extracts) in 1% Nonidet P-40 cell lysis buffer supplemented with protease inhibitors and deacetylase inhibitors cocktail (Santa Cruz Biotechnology) by following the procedures as previously described (Wang et al., 2009). Thirty micrograms of proteins of each sample were separated by 10% SDS-PAGE and electro-blotted to a nitrocellulose membrane in Tris-glycine buffer containing 20% methanol. The membrane was blocked with 5% skim milk in Tris buffered saline (TBS) for 1 h at room temperature and incubated with a primary antibody in TBS-T (TBS containing 0.05% Tween® 20) with 5% BSA overnight at 4°C. After washing with TBS-T, the membrane was incubated with horseradish peroxidase-conjugated secondary antibody diluted in TBS-T with 5% BSA for 45 min at room temperature. After four washes with TBS-T and one wash with TBS, the protein bands were visualized using ECL substrate and ChemiDoc Imaging System (Bio-Rad). The antibodies used were anti-histone (H)3, acetyl-H3 (Lys9/Lys14), HDAC1, HDAC2, IL-1 β , caspase-1, NLRP3, ASC (all from Cell Signaling Technology), GAPDH and β -actin (all from Santa Cruz Biotechnology).

Cell viability

Cell viability was determined by MTT colorimetric assay as previously described (Wang et al., 2009) by incubation of the cells with 10 μ l of MTT for each well for four hours followed by addition of 50 μ l of isopropanol with 0.04 N HCl to each well and reading the optical density at 570 nm with an ELISA reader. The results were expressed as optical density at 570 nm.

Determination of ASC oligomerization by Western blotting

ASC oligomerization was detected by western blotting as described previously (Lugrin and Martinon, 2017) with minor modifications. Briefly, 50 μ g of protein extracts were incubated with chemical crosslinker, DSP [dithiobis(succinimidyl propionate)] from ThermoFisher Scientific, at 2 mM at room temperature for 30 min with agitation on a rotator. The proteins were then centrifuged at 5,000x g for 10 minutes at 4°C. The pellets were collected and resuspended in SDS-PAGE sample loading buffer and treated at 100°C for 10 minutes before running SDS-PAGE and western blotting for ASC to determine the oligomerization of ASC using anti-ASC Ab. ASC levels in 30 μ g protein extracts without crosslinking were determined by western blotting as an input control of ASC oligomerization assay.

HDAC activity assay

Total HDAC activity was measured using an Epigenase HDAC Activity/Inhibition Direct Assay Kit (Colorimetric) (EpiGentek, NY, USA). For pan HDAC activities, the protein extracts prepared as described above were added into a 96-well ELISA plate coated with acetylated substrate peptide at 10 μ g protein in 49 μ l of HDAC assay buffer and 1 μ l of substrate per well in duplicates. For detection of specific HDAC activities, HDAC1, HDAC2 or HDAC3 were immunoprecipitated from 100 μ g of protein extracts using 4 μ l of specific Abs as described by us (Wang et al., 2012) using protein A/B plus agarose beads (Santa Cruz Biotech) after preclearing the proteins extracts with protein A/B plus agarose beads. The immunoprecipitated proteins were assayed for HDAC activity using equal volumes in HDAC assay buffer in duplicates. The plate with protein extracts or specific HDACs was incubated at 37°C for 90 minutes. The plate was washed and incubated with capture and detection Ab and developed following the protocol provided by the manufacturer. The activity of HDAC (OD/min/mg protein) was calculated according to manufacturer's specifications based on duplicate measurements of the optical densities at 450 nm.

Molecular docking studies

The structures of human HDAC1 and HDAC2 were downloaded from the Protein Data Bank (<https://www.rcsb.org>) with PDB IDs 4bkx.pdb and 3max.pdb for HDAC1 and HDAC2, respectively. The three-dimensional structure of DHOB was downloaded from PubChem (CAS 193551-00-7) in the form of sdf file and converted into pdbqt format as required by the docking software. The molecular docking studies were performed with AutoDock Vina (Trott and Olson, 2010) and the nine highest scoring binding modes for each

protein-inhibitor complexes that had the highest affinity and presumably strongest functional effects on the HDACs are illustrated in the results.

Drug affinity responsive target stability assay

Drug affinity responsive target stability (DARTS) was performed as described previously (Lomenick et al., 2009; Pai et al., 2015) with minor modifications. Briefly, 50 μ g of protein extracts of THP-1 cells were resuspended in 20 μ l of HBSS and the proteins were incubated with desired concentrations of DHOB or DMSO at the same dilution with DHOB as control at room temperature with shaking for 30 min. The proteins were then incubated with 40 ng of pronase diluted in 1 X TNC buffer (pH 8.0 50 mM Tris, 50 mM NaCl, and 1 mM calcium chloride) at the protein to pronase ratio of 1250:1 at room temperature for 25 mins. The digestion reaction was stopped by addition of equal volume of 2X SDS-PAGE sample loading buffer. The samples were treated at 70°C for 10 minutes before running for SDS-PAGE and western blotting detection of HDAC1, HDAC2 and HDAC3. The same membrane was stripped and blotted for GAPDH as control.

QUANTIFICATION AND STATISTICAL ANALYSIS

Normal distribution of data sets was evaluated using the Shapiro-Wilk normality test. Paired sample t-test analysis was used to evaluate differences between two experimental conditions using GraphPad Prism 8 software. P values below 0.05 were considered statistically significant.